

1 **Greenness, Nighttime Light, and Human Well-being**
2 - **Complex Nexuses Probed by Machines**
3

4 **Abstract**

5 The positive effects of greenness in living environments on human well-being are
6 known. As a widely used proxy, the nighttime light (NTL) indicates the regional socio-
7 economic status and development level. Higher development levels and economic status
8 are related to more opportunity and higher income, but NTL also causes light pollution and
9 other negative factors. However, the relationships between human well-being and
10 greenness and NTL remains inconclusive. Here, we demonstrate the complex nexuses
11 between subjective well-being (SWB) and greenness and NTL by employing the random
12 forest method. We apply the Shapley additive explanations (SHAP) to estimate the
13 contributions of greenness, NTL, and other features to SWB. Because SHAP is a
14 completely local way and cannot provide a general explanation, building connections
15 between feature values and their contributions is critical. We create a novel approach to
16 connect them on a geographical ground. Although overall greenness is positively
17 associated with SWB, while NTL is negatively linked, the relationships spatially vary. For
18 example, on average, the monetary value of a 1% increase in greenness on overall life
19 satisfaction (OVLS, an SWB indicator) is 120.94 (95%CI: 120.11 - 121.77) USD, while
20 the monetary value of NTL on OVLS is -833.96 (-956.85 - -711.08) USD/($nW/cm^2 \cdot sr$).
21 According to our results, greenness and NTL improvement should consider the local
22 environments rather than simply formulating one-size-fits-all policies or strategies. To

23 conclude, retaining a moderate development intensity and greening based on the local
24 status are necessary ways to achieve a sustainable society and improve human well-being.

25

26 **Keywords:**

27 Human Well-Being; NDVI; NTL; Environmental Valuation; Random Forest;
28 SHAP; Geographical Connection

29

30 **Introduction**

31 Greenness is positively associated with human well-being (Li and Managi 2021b;
32 MacKerron and Mourato 2013; White et al. 2013). Greenness leads to more recreational
33 and physical activities (Hunter et al. 2015), air pollution reduction (Eitelberg et al. 2016;
34 Li and Managi 2021a), relief of stress (Astell-Burt and Feng 2019; Astell-Burt et al. 2014;
35 Barton and Pretty 2010), among others. However, whether simple increases in greenness
36 would always give rise to improving human well-being remains inconclusive. In only terms
37 of the effects of greenness, seemingly, human well-being would be greater with more
38 greenness. Yet, the places with too much greenness do not have adequate land use for
39 infrastructure construction and developing economics, which would hurt human well-being
40 in a way. Previous studies show that people in Japan desire more urban land, especially in
41 metropolitan areas, due to crowded living environments (Li and Managi 2021b). Some
42 cities express the need for both urban land and natural land use. The contradiction between
43 green space and construction might be solved through moderate-intensity development and
44 population density reduction. Moderate-intensity development could leave a sufficient
45 amount of natural land use, making people live in cities naturally (Hartig and Kahn 2016).

46 Additionally, high development intensity is related to busy human activities, which
47 causes a series of environmental issues, such as light pollution (Falchi et al. 2011; Falchi
48 et al. 2019), traffic noise (Begou et al. 2020; Pirrera et al. 2010), among others. These
49 environmental issues lead to several detrimental effects on public health (Falchi et al. 2011;
50 Pirrera et al. 2010). The highly developed regions have more human activities and, in turn,
51 have more illumination. Thus, nighttime light (NTL) has long been widely used as a proxy
52 for socio-economic development with geographical information in environmental studies

53 (Chen and Nordhaus 2011; Yeh et al. 2020). The brighter NTL is not only observed by the
54 satellites but also sensed by sleeping or trying to sleep. In fact, lighting levels in highly
55 developed regions are much higher than the needs for their tasks, and these residual lights
56 ultimately affect wildlife and human health (Falchi et al. 2011). Without enough luminosity,
57 the regions might be unsafe and poorly developed, which slashes human well-being (Suk
58 and Walter 2019). Yet, the surplus of luminosity would induce health issues (Falchi et al.
59 2011). Therefore, similar to greenness in living environments, the NTL must also be within
60 a moderate range, not too dark or bright. The relationships between human well-being and
61 greenness and NTL should be complex, but relatively accurate knowledge of it is helpful
62 to achieve a sustainable society.

63 Previous studies have shown that subjective well-being (SWB) could objectively
64 indicate human well-being (Diener et al. 2018; Oswald and Wu 2010). To measure SWB,
65 three different approaches focusing on different aspects of well-being are widely
66 considered and accepted (Steptoe et al. 2015): life evaluation (Diener et al. 2018;
67 MacKerron 2012; Oswald and Wu 2010), hedonic well-being (Kahneman et al. 2004), and
68 eudemonic well-being. The life evaluation method extracts well-being from people's
69 thoughts about the quality or goodness of their overall life, which is most widely used in
70 previous studies on environmental issues (Diener et al. 2018; Ryff 2014). Hedonic well-
71 being focuses on emotions, and eudemonic well-being concentrates on sense of life. In this
72 study, four SWB indicators, overall life satisfaction (OVLS), relative life satisfaction
73 (RLS), overall happiness (OH), and relative happiness (RH), are considered. Among them,
74 OVLS and OH are the life evaluations of individual overall life, while RLS and RH are the

75 comparison of the life evaluation with the people in the local community. In our dataset,
76 all SWB indicators are 5-degree, from negative (1) to positive (5).

77 Previous studies mainly assume the relationships between human well-being and
78 greenness and NTL are linear, even though considering geographical locations or the time-
79 fixed effects within individuals (Ghosh et al. 2013; Li and Managi 2021b; White et al.
80 2013). Linear assumptions have a fatal shortcoming in that the effects do not vary
81 according to the current status. Due to scarcity value, the effects of increases in greenness
82 and NTL might be larger when the current value is low. When the greenness or NTL value
83 is too high, their effects on human well-being might be lower or even change direction. In
84 addition, based on linear assumptions, the accuracy of models is relatively low, generally
85 no greater than 20%, e.g., (Akpinar et al. 2016; Ambrey and Fleming 2014; Krekel et al.
86 2016). Hence, to perform highly accurate analyses, we should not directly assume the
87 relationship between human well-being and features of interest before the analyses.
88 Machine learning methods always build models of data without too many pre-assumptions.
89 The random forest, one of the machine learning methods, does not need to assume the
90 relationship owing to its non-parametric algorithm (Breiman 2001). To grasp the
91 relationships between human well-being and greenness and NTL, we employ over 380,000
92 observations and apply the random forest method to acquire the high-fit model. The
93 random forest is based on boosting technology. Simply speaking, the final results are
94 predicted by a bundle of weak learners, decision trees. In random forests, every decision
95 tree is also non-parametric, making it difficult to explain. Random forests are typically
96 model-agnostic, so we must use tools to make their results understandable. Shapley
97 additive explanations (SHAP) is a novel method to explain the local contribution of a

98 certain feature of a specific observation to the output variable (Lundberg et al. 2020). To
99 link the local contribution of the feature and the real feature value, we combine
100 geographical division by the random forest model and geographically weighted regression
101 to build geographically local connections between feature values and their Shapley values.
102 This innovative approach increases the practicality and interpretability of random forest in
103 geoscience.

104

105 **Materials and Methods**

106 ***Materials***

107 *Survey*

108 From 2015 to 2017, our team conducts three waves of nationwide surveys in Japan.
109 The survey covers almost 300,000 and obtains over 450,000 validated questionnaires. To
110 avoid interviewer bias and complete each wave within one month, we perform the surveys
111 via the Internet. Since our survey includes several sensitive questions, such as educational
112 background, personal income, employment, among others, the Internet-based approach
113 could reduce the probability of fake answers to some degree (Chapman et al. 2019; Li and
114 Managi 2021c). The respondents are randomly sampled according to the population
115 distribution. We obtain permission from the Japanese government to survey around
116 November each year. According to the related laws and regulations, we must complete the
117 survey during the appointed period, which is always four weeks around November. The
118 laws and privacy protection rules make directly acquiring the detailed respondents'
119 addresses difficult and illegal. However, we are legally permitted to obtain respondents'

120 residential postal codes, so we require the postal code in the survey. We use geometric
121 centers of postal zones from Google Geocoding API as the approximate addresses of the
122 respondents in the analysis. The respondents are from 54,144 postal zones. This survey
123 covers many healthy, demographic and socio-economic characteristics, such as mental
124 health status, self-reported health, age, gender, job, educational background, income,
125 among many others. After removing the observation with missing data, our datasets keep
126 more than 380,000 records. Although the random forest method could fill in missing data
127 (Breiman 2001), the computing time cost is vast and unacceptable. Thus, we drop these
128 missing data.

129

130 *Human Well-Being*

131 SWB is individuals' evaluation of their lives based on their own judgment and
132 experience (Diener 1984). The objective connection between SWB and objective living
133 conditions has been proved (Oswald and Wu 2010). This study uses four indexes to
134 represent SWB: OVLS, RLS, OH, and RH, which are widely employed and investigated
135 in SWB-related studies (Diener 1984; Diener et al. 2018). Generally, life satisfaction,
136 happiness, and Cantril's Ladder are regarded as evaluated SWB indicators individually.
137 OVLS and OH are the overall evaluation of the quality of life. RLS and RH are the
138 individual's life quality compared to people in your local community. We apply the
139 following questions for evaluating individual OVLS and RLS: "overall, how satisfied are
140 you with your life?" and "How satisfied are you compared to people in your local
141 community?". Then, the respondents should select an answer from "very satisfied (5)" to
142 "very unsatisfied (1)" for those two questions. To measure people's OH and RH, we ask

143 the respondents to answer following questions: “overall, how happy are you with your
144 life?” and “how happy are you compared to people in your local community?”. Similarly,
145 the potential answers for happiness-related questions are from “very happy (5)” to “very
146 unhappy (1)”. Here, it must be underscored that the OVLS, RLS, OH, and RH scores are
147 qualitative and ordinal rather than quantitative. Yet, our analyses are not classification tasks
148 because the output scores are not categorical. **Figure 1.a** illustrates the statistical
149 distribution of the SWB evaluation score, including OVLS, RLS, OH, and RH. Over
150 180,000 respondents deem that they are slightly satisfied with their lives overall, i.e., the
151 OVLS score is 4, which significantly exceeds other selections. Furthermore, approximately
152 210,000 respondents feel slightly happy with their life. The average values of RLS and RH
153 are relatively lower than the means of OVLS and RH. In this way, although more people
154 feel satisfied and happy in their own lives, they are rarely apt to feel they are better than
155 others.

156

157 *Normalized Difference Vegetation Index (NDVI) and Nighttime Light (NTL)*

158 To examine the impact of greenness on human well-being, we use the 16-day level
159 3 NDVI data with 500-m spatial resolution produced by the U.S. National Aeronautics
160 and Space Administration (NASA), which is widely used in previous environmental
161 research (Lamchin et al. 2018; Li et al. 2015; Wang et al. 2020). The NDVI is a graphical
162 index to describe whether the observed pixel contains live green vegetation and ranges
163 from -1 (no live green vegetation, -100%) to 1 (rife with live green vegetation, 100%)
164 (Didan et al. 2015). The NDVI data from NASA’s products, MOD13A1
165 (<https://lpdaac.usgs.gov/products/mod13a1v006/>) and MYD13A1

166 (<https://lpdaac.usgs.gov/products/myd13a1v006/>), are based on MODIS Terra and Aqua
167 Satellites, respectively. The period of interest is from October to December each year
168 because the survey is conducted around November. The MOD13A1 and MYD13A1's
169 temporal resolution is 16-day. NASA provides the data on the 289th, 305th, 321st, 337th, and
170 353rd in each year. We average the 16-day data in each year from Terra and Aqua into one
171 raster. Then, we take the geometric centers of postal zones as the center to build buffers
172 with a 5-km radius. The mean NDVI values of each buffer are extracted, which are
173 considered as the natural level of each postal zone. **Figure 1.b** demonstrates the statistical
174 distribution of the mean NDVI.

175 Human activities, local economic status, and the goodness of infrastructures are
176 associated with human well-being (Chen and Nordhaus 2011, 2019). The NTL remote
177 sensing data are widely applied to investigate human activities and economic status (Chen
178 and Nordhaus 2019; Chen et al. 2021; McCallum et al. 2022) because artificial electric
179 light is equipped in most buildings and infrastructures. The NTL data are extracted from
180 other NASA products, Suomi National Polar-orbiting Partnership Visible Infrared Imaging
181 Radiometer Suite (NPPVIIRS) nighttime light data. The earth observation group provides
182 monthly NTL data with a 1-km resolution. We calculate the average rasters of October's,
183 November's and December's data in each year and then extract the mean NTL values via
184 the buffers with a 5-km radius. The unit of NTL is nanowatt per square centimeter steradian
185 ($nW/cm^2 \cdot sr$). **Figure 1.c** shows the statistical distribution of the NTL.

186

187 *Demographic and Socio-economic Characteristics*

188 Several demographic and socio-economic characteristics are controlled, as in
189 previous studies (Krekel et al. 2016; Li and Managi 2021b, c; MacKerron and Mourato
190 2013). Our study is to probe the relationship between human well-being and living
191 environments, so the attitudes toward living environments, including the safe feeling of
192 living environments, the sense of goodness for living, and community attachment, are
193 analyzed. The frequency of high-level and low-level stress, the level of ease to relax, and
194 self-reported health represent health status. Gender, age, annual income, education
195 background (one-hot vector), and employment status (one-hot vector) are also employed
196 in the analysis. It must be noted that individual annual income in the survey is an income
197 range rather than an accurate overall income. In total, 29 features are considered in the
198 model (Descriptive statistics of the features are shown in **Appendix Table A1**).

199

200 **Methods**

201 *The Regression Decision Tree*

202 A decision tree is the basic element of the random forest method. The decision tree
203 predicts the output variable based on a series of judgments (Breiman 2001; Liaw and
204 Wiener 2002). Therefore, the decision tree is an entirely non-parametric approach. When
205 the output variable of the decision tree is categorical, the decision tree is to perform a
206 classification task and called a classification tree. If the output variable is continuous, the
207 decision tree is, in turn, named a regression tree. The difference between regression and
208 classification trees is how to process the predicted values in the end leaves. In the regression
209 tree, the predicted value is the mean of the output values remaining in the specific end leaf

210 from the training dataset, while the predicted value in the classification tree is the mode.
211 To analyze ordinal output variables, the previous studies mainly assume that they are
212 continuous and use a regression decision tree (Hothorn et al. 2006). **Figure 2** illustrates a
213 simple example of a regression decision tree with two layers. The algorithm should pass
214 two internodes and do two judgments to complete the prediction in the example tree. In the
215 example, two features, self-reported health, and NDVI, are used to predict individual SWB.
216 Self-reported health in this study is ordinal, and NDVI is continuous. In the training process,
217 the rules of each judgment and feature range splits are the primary things that the machine
218 needs to “learn”. A large amount of data is employed to train the decision tree to minimize
219 the residual sum of squares (RSS). The judgment rules and feature range splits that generate
220 the smallest RSS are the decided rules of the final model. We apply a greedy approach
221 based on the minimization of the RSS to train regression decision trees (Breiman et al.
222 2017):

$$RSS = \sum_{l \in leaves} \sum_{i \in C_l} (y_i - \bar{y}_{C_l})^2 \quad (1)$$

223 where l is a leaf, C_l is the cases in leaf l , y_i is the observed value and \bar{y}_{C_l} is the average
224 observed value in leaf l . In this approach, one feature might be split into several ranges
225 rather than only two. For example, the first internode might judge whether the NDVI
226 exceeds 30%, and the second internode might focus on whether the NDVI is more than
227 50%. The increase in the number of internode of trees would reduce the RSS. The division
228 would stop until the ending leaves are purified or the algorithm reaches the pre-defined
229 requirements. The unlimited number of internodes costs a huge amount of computer
230 memory, leading to calculation failure. We set the minimum number of samples required

231 to split an internal node ($N_{internal}$) as 100. Although using a smaller number could
232 improve the accuracy of models, the improvement is marginal in our training processing.
233 Keeping other settings the same, changing the setting of the $N_{internal}$ from 100 to 1 could
234 only improve 0.2% in R^2 . If $N_{internal}$ is smaller than 100, the further split stops in a
235 certain branch.

236

237 *Random Forest*

238 A single regression decision tree is insufficient to accurately predict the output
239 variables. In most regression tasks, decision trees are usually deemed as weak learners due
240 to their relatively lower goodness of fit and flexibility. However, they are good at grasping
241 the non-linear relationship compared with the other regression methods. In order to
242 improve the accuracy and keep the advantage of the decision tree, the random forest
243 method is created (Breiman 2001). Random forest ensembles hundreds of decision trees,
244 lets them individually predict the results, and averages all the predicted results from each
245 tree. This is typically boosting technology, which aims to use a set of weak learners to
246 create a strong learner (Schapire 2003). Bootstrapping and bagging are the key
247 technologies to improve the accuracy and reliability of the random forest (Liaw and Wiener
248 2002). Bootstrapping is the sampling technology, which is randomly sampling with
249 replacement. This technology allows features with almost any statistical distribution to be
250 used in the analysis. To process bootstrapping, the number of trees (N_{tree}) in the random
251 forest should be set. The N_{tree} sub-samples with replacement are extracted from the total
252 sample. The sizes of each sub-sample are 2/3 of the total sample size. Every decision tree
253 is trained by the bootstrapped sub-sample. It should be emphasized that only a fixed

254 maximum number of random features ($N_{feature}$) are employed in a single decision tree,
255 rather than all. After training, the random forest can predict the output variable by
256 aggregating the predicted results from each tree. The process that uses the bootstrapped
257 data set and aggregates the predicted results from each tree is terminologically named
258 “bagging”. Because each tree only uses 2/3 data in the bagging, the remaining data are
259 called out-of-bagging (OOB) data. The OOB data are applied to test the accuracy of models.
260 OOB data are employed to calculate the OOB score, which is the accuracy of OOB data
261 caused by the trained random forest. This process is similar to cross-validation but has been
262 assembled in the random forest method.

263 Several parameters including N_{tree} , $N_{feature}$, and $N_{internode}$, in our random
264 forests need to be pre-defined. The accuracy of the random forest will enhance with the
265 number of trees increasing. However, the benefit from the increase in the tree number
266 gradually becomes marginal. According to our experience, the random forest with 1,000
267 trees could improve the model accuracy to a stable level, so the N_{tree} is set to 1,000 in our
268 models. Additionally, previous studies and the method designer recommend the feature
269 number employed in each tree should be 1/3 of all features in the original data set for
270 regression tasks (Breiman 2001; Breiman et al. 2017; Liaw and Wiener 2002). We compare
271 the cross-validation scores of the models with different numbers of features to maximize
272 the model accuracy. According to the cross-validation, the optimal models’ $N_{feature}$ are 7.
273 A relatively larger $N_{internode}$ leads to the accuracy reduction and smaller size of the model.
274 Balancing the memory consumption and model accuracy, we set $N_{internode}$ to 100.

275 Compared with typical linear regression methods widely applied in previous studies,
276 such as ordinary least square (OLS) and ordered logit regression (OLR), the random forest

277 has an obvious advantage in that this method does not need to assume the linear
278 relationships between output variables and features. In fact, relationships in the real world
279 are normally more complex than linear. For example, the relationship between NDVI and
280 human well-being might not be linear. Without any greenness in living environments,
281 humans might feel unhappy. In this case, the association is positive. However, if the
282 residential area fills with only greenness, that would be deemed as an entirely undeveloped
283 area. Living in an undeveloped area, humans might also feel uncomfortable. Now, the
284 relationship becomes negative. If we assume a linear relationship, the conclusions might
285 be misleading. Furthermore, the regression methods based on the matrix approach to
286 estimate the coefficients, such as OLS and OLR, must avoid multicollinearity in the
287 analyses. In real-world situations, many variables represent completely different data but
288 are highly correlated. In the OLS or OLR, we need to drop some variables to guarantee no
289 correlation between independent variables exists. This variable selection process is
290 unnecessary in the random forest because this model does not require the features to be
291 independent and identically distributed.

292 Whether the features of interest are significantly important to the random forest
293 model is a critical question. The random forest model estimates the feature importance by
294 computing the change in model accuracy before and after permutating a certain feature
295 (Breiman 2001). A big change means that the removed feature is vital to predicting the
296 output variables because the sum of residuals increases significantly with this feature. For
297 example, if the accuracy of a model with all features is 40% and after removing a feature
298 of interest, the accuracy reduces to 20%, the importance of the removed feature is 0.5. In
299 this study, the importance of a feature ranges from 0 to 1.

300

301 *Shapley Additive Explanations (SHAP)*

302 Despite the high accuracy achieved by the random forest algorithm in many
303 applications, it can be difficult to interpret and explain the outcomes due to the complexity
304 of the model (Friedman 2001; Greenwell 2017; Lundberg et al. 2020). SHAP is an
305 advanced interpretability technique that helps explain each feature's contribution locally
306 by using the concept of Shapley values (Lundberg and Lee 2017). In this method, each
307 feature of the observation is treated as a “player” in a game, where the prediction value is
308 the payout. The Shapley values are used to allocate the payout fairly among the players,
309 resulting in a clear understanding of the individual impact of each feature on the model’s
310 output (Lundberg and Lee 2017; Molnar 2020). In other words, the Shapley values are the
311 fair contributions of a certain feature to the output. Firstly, the contribution should be
312 estimated as follows:

$$g_i^j(x) = E(f(\mathbf{X}) \mid \mathbf{X}^1 = x^1, \dots, \mathbf{X}^{j-1} = x^{j-1}, \mathbf{X}^j = x^j) - E(f(\mathbf{X}) \mid \mathbf{X}^1 = x^1, \dots, \mathbf{X}^{j-1} = x^{j-1}) \quad (2)$$

313 Where x represents a certain observation, i represents a particular feature of interest,
314 $g_i^j(x)$ represents the contribution of the feature i of the observation x take the feature i as
315 the j -th feature, \mathbf{X} represents a matrix of random values of features, $f()$ represents our
316 trained random forest model, x^1, \dots, x^{j-1} are a permutation of other features except the
317 feature i , $\mathbf{X}^1, \dots, \mathbf{X}^{j-1}$ are the columns corresponding to x^1, \dots, x^{j-1} in \mathbf{X} ,
318 $E(f(\mathbf{X}) \mid \mathbf{X}^1 = x^1, \dots, \mathbf{X}^{j-1} = x^{j-1}, \mathbf{X}^j = x^j)$ is the expected value of the predictions of \mathbf{X} ,
319 when we set $\mathbf{X}^1 = x^1, \dots, \mathbf{X}^{j-1} = x^{j-1}, \mathbf{X}^j = x^j$, and $E(f(\mathbf{X}) \mid \mathbf{X}^1 = x^1, \dots, \mathbf{X}^{j-1} = x^{j-1})$

320 is the expected value of the predictions of \mathbf{X} , when we set $\mathbf{X}^1 = x^1, \dots, \mathbf{X}^{j-1} = x^{j-1}$. Here,
 321 $g_i^j(x)$ is affected by j . For example, $g_i^{j=2}(x)$ and $g_i^{j=3}(x)$ are not the same, even though
 322 they are both the estimated contribution of feature i of the observation x . To estimate the
 323 contributions stably and fairly, the Shapley value averages all potential contributions of the
 324 feature i of the observation x as follows:

$$S_{ix} = E\left[\frac{1}{p!} \sum_J g_i^{j|\pi(J,j)}(x)\right] \quad (3)$$

325 where S_{ix} represents the Shapley value of the feature i of the observation x , J represents a
 326 permutation of the set of indices $\{1, 2, \dots, p\}$ corresponding to an ordering of p features
 327 included in our random forest model (in total, there are $p!$ potential permutations), $\pi(J,j)$
 328 represents the set of the indices of the features contained in J before the feature i at position
 329 j , and $g_i^{j|\pi(J,j)}(x)$ represents the estimated contribution value of feature j of the
 330 observation x with a specific permutation in $\pi(J,j)$. It is important to note that random
 331 values are typically not considered informative in explaining a model's behavior. In
 332 practice, the random dataset \mathbf{X} used in computations is not generated randomly but rather
 333 chosen randomly from our dataset. To optimize computation time, we followed the
 334 recommendation of the Python package makers and set the dataset size of \mathbf{X} to 1000
 335 (Lundberg et al. 2020). A larger dataset size would significantly increase computation time.
 336 To efficiently estimate the Shapley values, we used 4048 random permutations of all
 337 features. While more permutations would improve the accuracy of the estimated values,
 338 the computational cost is prohibitive

339

340 *Geographical Connection between Reality and Explanation*

341 The explanations based on the Shapley values are entirely local. The Shapley value
342 of a certain feature of a specific observation is generally different from the other
343 observations', even though the values of the feature of interest are the same. In other words,
344 the Shapley values of one respondent's features only explain her/his situation and cannot
345 be directly applied to interpret others' situations. However, we need a general estimation
346 to help the government and society formulate environmental strategies and policies. Hence,
347 the connections between feature values, which represent reality, and their Shapley values,
348 which indicate explanations, are necessary. The simplest way is to build a linear regression
349 model between the feature values and their Shapley values. Based on the linear connection,
350 a certain feature value's contribution to SWB could be easily estimated. This method has
351 some disadvantages. Because this research covers the whole of Japan, a unified relationship
352 is suspicious in terms of the individual-level study on a huge spatial extent. Using spatially
353 local relationships to link reality and explanation is more valid.

354 The key aspect of the spatially local method involves creating a series of spatially
355 local datasets. During the model training process, location information, specifically the
356 longitude and latitude of the observation, is included. Some decision trees are designed to
357 incorporate these features, dividing the global extent into multiple zones. The observation's
358 location is assigned to the zones created by different trees, and a bag of boundaries is
359 obtained. The maximum values of the boundaries in each direction are considered as the
360 dividing lines. As a result, every observation is surrounded by a rectangle of dividing lines,
361 and the neighbors are those located within the zone. Since the neighbor zones differ
362 between locations, the local relationship is estimated using one observation and others

363 located in its neighbor zone. The relationship coefficients vary spatially based on the
 364 location of the center observation. The spatially local coefficient is estimated as follows:

$$S_{ix}^l = \alpha_{ix} X_{ix}^l + \beta_{ix} + e_{ix} \quad (4)$$

365 where α_{ix} and β_{ix} are the slope and the intercept of the local relationship between feature
 366 i 's value and its Shapley value based on x 's neighbor zone, l is the local dataset taking x
 367 as the center observation, X_{ix}^l is a vector of the feature i 's values in x 's neighbor zone in
 368 local dataset l , and S_{ix}^l is a vector of the Shapley values corresponding to X_{ix}^l . Using the
 369 local relationship coefficients makes it possible to interpret the marginal contribution of a
 370 specific feature to SWB to a specific geographical extent. We utilize geographical weights
 371 to improve the continuity of the links between features and their Shapley values. This helps
 372 us better understand the spatial variations in the impact of the features on SWB and identify
 373 improvements for specific geographic areas. We calculate the local geographical weight
 374 vector as geographically weighted regression methods (Li and Managi 2021c, 2022) as
 375 follows:

$$\mathbf{W}_x = [1 - (\mathbf{d}_x/h_x)^2]^2 \quad (5)$$

376 when \mathbf{W}_x is geographical weight vector of the elements in x 's neighbor zone, \mathbf{d}_x is a
 377 vector of distances between x and the elements in x 's neighbor zone, and h_x is the furthest
 378 distance of the vector \mathbf{d}_x . The elements in x 's neighbor zone that are furthest away always
 379 have zero weights. On the other hand, the observation x itself always has the highest weight
 380 of 1 in the regression. The geographically weighted coefficients are estimated as follows:

$$Coef_{ix} = (X_{ix}^{l^T} \mathbf{W}_x X_{ix}^l)^{-1} X_{ix}^{l^T} \mathbf{W}_x S_{ix}^l \quad (6)$$

381 where Coef_{ix} is the estimated local coefficients, including α_{ix} and β_{ix} . Here, the slope of
 382 the local regression, α_{ix} , could be regarded as the marginal effect of a certain feature i on
 383 SWB.

384 The local coefficients, Coef_{ix} , could not only represent the relationship between
 385 feature i and SWB of the observation x 's location, but also the x 's neighbor zone. The
 386 neighbor zones of each observation overlap. **Figure 3** is a schematic diagram of
 387 overlapping. In **Figure 3**, there are three neighbor zones of the observations, x_1 , x_2 , and
 388 x_3 . Due to overlapping, the whole area is divided into seven zones from A to G. The zones
 389 A, B, and C belong to only one neighbor zone individually, so their local coefficients equal
 390 to Coef_{ix1} , Coef_{ix2} , and Coef_{ix3} . The coefficients of the zones D, E, F, and G should be
 391 the average value of local coefficients belonging to the neighbor zones. For example, we
 392 use the following process to estimate the local coefficient of zone D, Coef_{iD} :

$$S_{ix1} = \alpha_{ix1}x + \beta_{ix1}$$

$$S_{ix2} = \alpha_{ix2}x + \beta_{ix2}$$

$$S_{iD} = (S_{ix1} + S_{ix2})/2 \quad (7)$$

$$\alpha_{iD} = (\alpha_{ix1} + \alpha_{ix2})/2$$

$$\beta_{iD} = (\beta_{ix1} + \beta_{ix2})/2$$

393 where S_{ix1} , S_{ix2} , and S_{iD} are the estimated Shapley values of the feature i based on the
 394 relationships in the neighbor zones of observation x_1 , x_2 , and the zone D, α_{ix1} , α_{ix2} , and
 395 α_{iD} are the slopes of the relationships between the feature i and its Shapley value, β_{ix1} ,
 396 β_{ix2} , and β_{iD} are the intercepts of the relationships between the feature i and its Shapley
 397 value, and x is the value of feature i in zone D. α_{iD} is called as geographically average

398 effects of feature i on SWB in zone D. In order to make the research results easier to
399 understand and apply by the government and the public, the local coefficients in the
400 overlapped neighbor zones are processed following the abovementioned method.

401

402 *Monetary Values of Features*

403 To make the impacts of features of interests on SWB understandable and
404 comparable, we estimate their monetary values. We take the marginal substitution rate
405 (MSR) of features of interest and income as the monetary values (Krekel et al. 2016; Li
406 and Managi 2021b, c). The SWB variation of the change in the feature of interest should
407 be offset by the income improvement. According to the local linear relationships, a 1-unit
408 increase in a certain feature would change SWB, since the feature's contribution, Shapley
409 value, varies based on the current status. If no variation in SWB is needed, the shift in
410 income is assumed. The amount of income change is deemed as the monetary value of a 1-
411 unit increase in a certain feature. The monetary value of the certain feature is estimated as
412 follows:

$$MSR_{iz} = \frac{\alpha_{iz}}{\alpha_{INCz}} \quad (8)$$

413 where MSR_{jx} is the MSR of the feature i in the zone z , and α_{INCz} is geographically
414 average effects of income on SWB in zone z , and α_{iz} is geographically average effects of
415 feature i on SWB in zone z .

416

417 **Results**

418 We build four random forest models with 1,000 decision trees for OVLS, RLS, OH,
419 and RH, respectively. The R^2 , mean square error (RMSE), mean absolute error (MEA),
420 and cross-validation score (CV score) of the random forest models are compared with the
421 indicators of the regression model, OLS (**Table 1**). For random forest models, the OOB
422 scores are considered as CV scores, while the average values of 10-fold cross-validation
423 are the CV scores for OLS. The better models have higher R^2 , higher CV scores, lower
424 RMSE, and lower MAE. In terms of accuracy, the random forest models are significantly
425 better than the linear regressions. The accuracy of models in this study is better, which is
426 always higher than 40%, while the model accuracy is generally lower than 20% in previous
427 studies regarding the relationships between environments and SWB, e.g., (Akpinar et al.
428 2016; Bertram and Rehdanz 2015; Krekel et al. 2016).

429

430 ***Feature Importance***

431 **Figure 4** illustrates the importance of features in four random forest models. In all
432 models, the feature, easy to relax, is the most important. Furthermore, the frequency of
433 high-level stress and low-level stress also affect SWB significantly. In total, mental health
434 is closely related to SWB, consistent with previous studies (Diener et al. 2018), since the
435 sums of the importance of mental-health-related features exceed 0.3 in four models.
436 Another feature depicting physical health, self-reported health, is apparently linked to SWB,
437 contributing more than 0.05 to the model accuracy. The living-environment-related
438 features, including goodness for living, living environment safety, and community

439 attachment, provide over 0.2 accuracies for each model. Two income-related features,
440 income level and individual income, contribute more than 0.05 to the model accuracy, and
441 their contributions are always the same because individual income is converted from
442 income level. NDVI's and NTL's importances are more than 0.02 individually in each
443 model. The importance of the feature, year, could illustrate temporal stability. For OH and
444 RH, the importance of year are lower than 0.02, while it is greater than 0.03 for OVLS and
445 even reaches approximately 0.13 for RLS. In this way, the difference in RLS over three
446 years is significant. In other words, RLS is not as temporal stable as other SWB indicators.

447

448 ***Global Linear Connection Results***

449 The means of the Shapley values of NDVI for OVLS, RLS, OH, and RH are
450 1.46×10^{-4} , 2.42×10^{-4} , -0.40×10^{-4} , and 1.28×10^{-4} , respectively. Most SWB
451 indicators benefit from the current NDVI status except OH. In terms of global linear
452 relationships between NDVI and SWB, an increase in NDVI is related to SWB
453 improvement because the coefficients of the linear regressions between NDVI and OVLS,
454 RLS, OH, and RH are significantly positive, which are 2.34×10^{-4} (p-value < 0.1%),
455 1.73×10^{-4} (p-value < 0.1%), 2.47×10^{-4} (p-value < 0.1%), and 2.32×10^{-4} (p-
456 value < 0.1%), respectively. The linear coefficient can be understood as the marginal effect
457 of increased NDVI on SWB. For example, a 1% increase in NDVI is associated with a
458 2.34×10^{-4} increase in OVLS. However, R²s of the global linear relationships are
459 relatively low, which are 23.30%, 14.04%, 26.45%, and 23.67%. Hence, in this study, the
460 global relationships demonstrate the tendency between NDVI and its contribution, while
461 spatially local connections depict concrete and accurate relationships. Mental health affects

462 the contribution of greenness to SWB, illustrated by **Figures 5, 6, and 7**. People who are
463 difficult to relax, with a high frequency of high-level stress, and with a high frequency of
464 low-level stress, are more sensitive to greenness in their living environments because the
465 Shapley values of their NDVI are relatively extreme. With negative psychological statuses,
466 low NDVI extremely slashes SWB, whereas those people benefit more from high NDVI
467 (**Figures 5, 6, and 7**). The relationship between NDVI and its contributions is less impacted
468 by other features.

469 The means of the Shapley values of NTL for OVLS, RLS, OH, and RH are
470 -2.18×10^{-4} , -3.32×10^{-4} , -2.81×10^{-4} , and -3.88×10^{-4} , respectively. People
471 are apt to be unsatisfied with the NTL in their living environments. The negative global
472 linear relationships are significant as the coefficients between NTL and its contributions to
473 OVLS, RLS, OH, and RH are -2.34×10^{-4} (p-value < 0.1%), 1.73×10^{-4} (p-value <
474 0.1%), 2.47×10^{-4} (p-value < 0.1%), and 2.32×10^{-4} (p-value < 0.1%), respectively.
475 The coefficients should be explained as the effect of a $1-nW/cm^2 \cdot sr$ increase in live
476 environment NTL on SWB. The accuracy of global linear relationships between NTL and
477 SWB are relatively higher, which are 74.83%, 53.42%, 69.61%, and 71.98%, individually.
478 Similar to NDVI, the relationship between NTL and its contributions to SWB are also
479 easily impacted by mental health, shown in **Figure 8, 9, and 10**. People with difficulty to
480 relax, higher frequency of high-level stress, and/or higher frequency of low-level stress
481 tend to benefit more from the lower NTL. The poor mental health status aggravates the
482 negative effects of higher NTL on SWB.

483 The average Shapley values of individual income for OVLS, RLS, OH, and RH are
484 -2.00×10^{-3} , -1.52×10^{-3} , -1.58×10^{-3} , and -1.85×10^{-3} , respectively. To

485 most people, current individual income has a negative contribution to SWB. In the global
486 estimations, the slopes between individual income and OVLS, RLS, OH, and RH are
487 significantly positive, which are 1.45×10^{-2} (p-value < 0.1%), 1.15×10^{-2} (p-value <
488 0.1%), 1.11×10^{-2} (p-value < 0.1%), and 1.22×10^{-2} (p-value < 0.1%), respectively.
489 The accuracies of the global linear regression for OVLS, RLS, OH, and RH are 73.32%,
490 77.40%, 66.31%, and 76.58%, individually.

491

492 ***Geographically Local Linear Relationship***

493 Using the geographical connections between feature values and their Shapley
494 values, the accuracy of relationships increases. The R^2 s of the local linear relationships
495 between NDVI and its contributions to OVLS, RLS, OH, and RH, are 30.46%, 31.58%,
496 32.33%, and 39.25%, respectively. The accuracy of the geographically local relationships
497 between NTL and its contributions to OVLS, RLS, OH, and RH increases to 78.46%,
498 62.20%, 71.92%, and 80.91%. The accuracy of local links between individual income to
499 its Shapley value on SWB indicators reaches 75.28%, 79.05%, 68.77%, and 80.91%,
500 individually. In fact, reducing the local datasets could further improve accuracy. For
501 example, in the current local dataset division, if a single tree considers two locations in the
502 same divided range, those two locations are deemed as neighbors. In this way, every local
503 dataset has the most amount of observations. However, if we require the neighbor
504 definition must be accepted by most trees, the sizes of local datasets become smaller. The
505 geographical coefficients are more local, and the accuracy will increase. The cost is the
506 reduction in the continuity and coverage of geographically local relationships. In this study,

507 we prefer to obtain the largest explained areas, so we use the most lenient requirement to
508 define the neighbor zone.

509 To illustrate the effects of NDVI, NTL, and income as widely as possible, we
510 convert the geographically local relationships into the geographically average effect of
511 NDVI, NTL, and income on SWB. It must be emphasized that simply plotting the local
512 coefficients would be hard to read because they are points and overlap a lot. **Figures 11,**
513 **12, 13, and 14** demonstrate the spatial distribution of the geographically average effect of
514 NDVI on OVLS, RLS, OH, and RH, respectively. The accuracy of the geographically
515 average effect of NDVI on SWB slightly decreases compared with the accuracy of local
516 linear relationships, which are 29.73%, 30.61%, 29.94%, and 37.94%, respectively. Based
517 on the spatial distribution of the geographically average effect of NDVI on SWB, the
518 relationships between NDVI and its contributions to SWB are not globally unified. The
519 degree and even direction of the effects spatially vary. For instance, in **Figure 11**, in most
520 areas, the effects of the increased NDVI on OVLS are positive, but in some metropolitan
521 areas, such as Tokyo and Nagoya, the effects of NDVI are negative. In some metropolitan
522 areas, an increase in greenness cannot improve OVLS and even harms it. In Hokkaido, the
523 increased greenness could improve OVLS, OH, and RH, but reduce RLS. In rural areas, an
524 increase in greenness negatively affects OVLS, and OH (**Figures 11 and 13**).

525 The geographically average effects of NTL on SWB are illustrated in **Figures 15,**
526 **16, 17, and 18.** The accuracy of the geographically average effects of NTL on OVLS, RLS,
527 OH, and RH is 76.07%, 61.63%, 71.62%, and 80.08%, respectively. Overall, an increased
528 NTL is harmful to SWB in most areas. NTL is usually taken as the development index in
529 previous studies (McCallum et al. 2022; Zhao et al. 2022), but the extremely bright light

530 during the night to the residents is adverse, such as light pollution (Suk and Walter 2019).
531 As a direct factor, the NTL might have a negative effect on SWB. In metropolitan areas,
532 the negative impacts of the increased NTL are relatively slight. **Figures 19, 20, 21, and 22**
533 show the geographically average effects of income on four SWB indicators. Their accuracy
534 is 74.74%, 78.60%, 68.14%, and 78.01%, respectively. Almost in all places, the increased
535 income's effects are positive to all SWB indicators.

536

537 ***Monetary Values***

538 **Figures 23, 24, 25, and 26** illustrate the monetary value of a 1% increase in NDVI
539 in the living environments on OVLS, RLS, OH, and RH. The monetary values of NDVI in
540 the figures were converted into US dollars in 2015. The distributions of NDVI's monetary
541 values are similar to the distribution of the geographically average effects of NDVI, since
542 the geographically average effects of income are almost in the same direction, and the
543 numerical variations of them are relatively tiny. The average monetary value of NDVI on
544 OVLS of all observations' locations is 120.94 USD/%, whose 95% confidence interval (95%
545 CI) is from 120.11 to 121.77 USD/>. The average monetary values of NDVI on RLS, OH,
546 and RH are 60.31 (95% CI: 55.73 – 64.90) USD/%, 191.85 (95% CI: 190.91 – 192.80)
547 USD/%, and 89.44 (95% CI: 87.43 – 91.46), respectively. Greenness mainly improves
548 happiness more, especially OH. **Figures 27, 28, 29, and 30** demonstrate the monetary value
549 of a $1-nW/cm^2 \cdot sr$ increase in NTL in living environments on four SWB indicators. The
550 average monetary values of a $1-nW/cm^2 \cdot sr$ increase in NTL in living environments on
551 OVLS, RLS, OH, and RH are -833.96 (-956.85 - -711.08) USD/($nW/cm^2 \cdot sr$), -819.59
552 (95% CI: -912.42 - -726.76) USD/($nW/cm^2 \cdot sr$), -846.10 (95% CI: -905.09 - -793.11)

553 USD/%, and -1541.05 (95% CI: -1695.92 - -1386.18), respectively. The increased NTL
554 harms RH the most, compared with other SWB indicators.

555

556 Discussion

557 This study is the first study employing the random forest model, SHAP, and
558 geographical connection between features and their contribution to the output variable. We
559 directly take the observations' location information, including longitude and latitude, into
560 the random forest model, which is an important attempt to apply machine learning to a
561 geographical topic. The "random" division of geographical extent in the random forest
562 provides a novel approach to defining the neighbor zones, different from the traditional
563 way based on distance or sharing boundary (Beenstock and Felsenstein 2019;
564 Fotheringham et al. 2002). The "random" division could guarantee that the people with
565 similar features living close to each other are put into the same group (the end leaf in
566 random forest terminology). The greedy division strategy maintains a lower RSS and
567 improves rationality of the "random" division. SHAP is a new method to explain the
568 random forest results (Lundberg et al. 2020), but the explanation is completely local.
569 Combined with geographical division by the random forest model and geographically
570 weighted regression, we build geographically local connections between features and their
571 Shapley values. Compared with a global linear connection, the geographically local link
572 avoids assuming a strong monotonous relationship globally and accepts that the
573 relationship could spatially vary. Additionally, the local connection usually has higher
574 accuracy. Finally, our method makes the spatial variation of the connections continuous.

575 Our main findings are that the relationships between SWB and greenness are
576 positive on average and in most places, whereas an increased NTL negatively impacts four
577 SWB indicators. Numerous previous studies have proved that greenness is positively
578 associated with human well-being (Li and Managi 2021b; MacKerron and Mourato 2013;
579 Tsurumi et al. 2018). People do benefit from a rational level of greenness because
580 greenness could provide recreational activities (MacKerron and Mourato 2013), air
581 pollution reduction (Chameides et al. 1988; Eitelberg et al. 2016; Mendoza-Ponce et al.
582 2018), and the creation of aesthetic, artistic, and scientific values for human beings (Felipe-
583 Lucia et al. 2018; Seresinhe et al. 2015). Counterintuitively, in some metropolitan areas,
584 including Tokyo and Nagoya, the increased greenness is negatively associated with the
585 SWB indicators. Intuitively, people in metropolitan areas with less greenness should desire
586 greenness. The possible explanation is that convenient transportation in the metropolitan
587 areas increases the accessibility of the natural environment, which fulfills the need for
588 greenness in living environments. Although more greenness might not directly reduce
589 human well-being, the land use for construction and development is significantly
590 insufficient. Previous study indicates that the people in Tokyo desire more urban land due
591 to crowded living environments (Li and Managi 2021b). In a sense, the direct impacts of
592 greenness on human well-being are overemphasized, whereas its indirect effects are not
593 well-researched or even ignored. In this study, the relationship between greenness and
594 human well-being is complex and varies spatially. Moreover, people with poor mental
595 health are more sensitive to the environment, which is the by-product of this study.
596 Previous studies claim that exposure to green spaces is linked to better mental health
597 (Bratman et al. 2019; Triguero-Mas et al. 2015). In other words, people with mental

598 disorders prefer to live in more comfortable environments. To make city development
599 sustainable, a simple increase in greenness cannot balance development and the
600 environment in terms of human well-being improvement. A reasonable greenness level is
601 linked to at least two sustainable development goals: good health and well-being (SDG3)
602 and sustainable cities and communities (SDG11). Therefore, efficient and effective usage
603 of the natural capital is a sustainable pathway to further improving human well-being in
604 Japan.

605 NTL is an essential indicator representing economic status and human activities
606 (Chen and Nordhaus 2011, 2019; Zhao et al. 2017). The correlation between luminosity
607 data and the regional GDP is significantly positive (Chen and Nordhaus 2011). The places
608 are brighter where the development level and economic status are better. The highly
609 developed areas have more opportunities and relatively higher incomes, so people there are
610 more likely to have greater human well-being. Sufficient NTL could provide safe feelings
611 for residents during the night (Gaston et al. 2015). For this reason, in rural areas without
612 enough illumination, the increased NTL could be a positive factor. However, the adverse
613 impacts of NTL on human health are rarely mentioned. Light pollution causes poor health
614 (Falchi et al. 2011; Falchi et al. 2019). Busy human activities are associated with more
615 noise, especially nocturnal road traffic noise. Primary sleep disturbances, cardiovascular
616 diseases, among others, are partially attributable to the detrimental effects of noise (Begou
617 et al. 2020; Pirrera et al. 2010). For all these reasons, the impact of an increase in NTL
618 should be negative. Intriguingly, the negative effects of NTL are relatively slight in
619 metropolitan areas because the adverse impacts on health could be offset by developed
620 environments with convenience and opportunity. To sum up, in poorly developed areas,

621 more NTL is connected to the improved safety feeling, which leads to improvements in
622 SWB. In relatively developed areas, the NTL might disturb residents' daily life, and the
623 development level of the community cannot compensate for the harmful impacts, so the
624 NTL effects are significantly negative. In metropolitan areas, the impacts of NTL are close
625 to zero because people are apt to accept both the negative and positive effects of high-level
626 NTL. Therefore, development planning should balance the development level and its
627 impacts on human well-being to achieve a sustainable society.

628 There are several limitations and issues worthy of note. First, geographically
629 uneven sampling makes the results look suspicious. In the metropolitan area, more people
630 are sampled since the sampling is according to population distribution. Moreover, the
631 residential locations are based on centroids of the postal zones. The postal zones are smaller
632 in densely populated areas, whereas they are larger in rural areas. This might aggravate the
633 spatially uneven distribution. Second, although this study employs a short panel data set,
634 the time-fixed effects within individuals are not considered. To the best of our knowledge,
635 few studies discuss whether and what data transformations are needed for panel regression
636 random forest. Third, more features should be put into the analysis. Although we have used
637 more features than in previous studies, other features, such as marital status, general health
638 questionnaire score, among others, are still unavailable. Finally, the output variables, the
639 SWB indicators, have too few degrees. An increase in the number of SWB evaluation
640 selections could further increase the accuracy of the analysis. In further studies, the random
641 forest model should be optimized to make it able to grasp the time-fixed within individuals.
642 Moreover, the causal relationships between human well-being and greenery and NTL are
643 desired.

644

645 Conclusion

646 The global relationship between SWB and greenness is positive, whereas the
647 connection between SWB and NTL is negative. However, simple increases in greenness or
648 decreases in NTL in living environments without considering the status quo do not always
649 improve human well-being. Although the geographically local relationships are not unified,
650 the average monetary values of greenness in the living environments on OVLS, RLS, OH,
651 and RH are 120.94 (95%CI: 120.11 - 121.77) USD/%, 60.31 (95% CI: 55.73 – 64.90)
652 USD/%, 191.85 (95% CI: 190.91 – 192.80) USD/%, and 89.44 (95% CI: 87.43 – 91.46),
653 respectively. The average monetary values of NTL are -833.96 (-956.85 - -711.08)
654 USD/(nW/cm² · sr), -819.59 (95% CI: -912.42 - -726.76) USD/(nW/cm² · sr), -846.10
655 (95% CI: -905.09 - -793.11) USD/(nW/cm² · sr), and -1541.05 (95% CI: -1695.92 - -
656 1386.18) USD/(nW/cm² · sr), individually. Our study illustrates the high-accuracy
657 relationship between human well-being and greenness and NTL to provide more
658 information for governments and the public. This essential information helps to formulate
659 sustainable land use and development policies to improve human well-being.

660

661 Data Availability

662 The fully reproducible codes are publicly available at
663 https://github.com/MichaelChaoLi-cpu/Greenness_NighttimeLight_WB.git. Data are
664 available from the corresponding author on reasonable request.

665

666 **Acknowledgment**

667 This research was supported by the following funding agencies: JSPS KAKENHI
668 (Grant No. JP20H00648), the Environment Research and Technology Development Fund
669 of the Environmental Restoration and Conservation Agency of Japan (Grant No.
670 JPMEERF20201001), and also JST SPRING (Grant No. JPMJSP2136).

671

672

673

674 **Table:****Table 1: Accuracy Statistical Indicators**

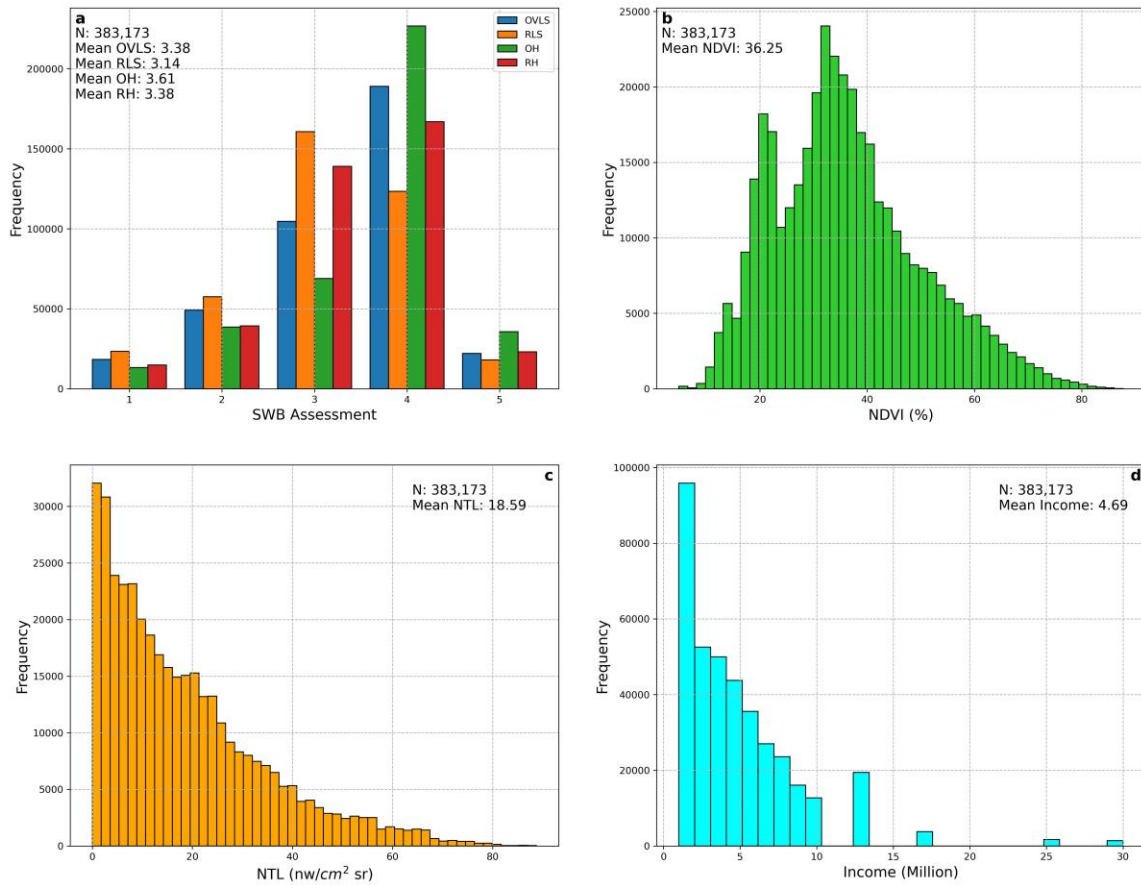
Output	Model	R ²	RMSE	MAE	CV score
OVLS	RF	44.95%	0.702	0.540	36.71%
	OLS	34.61%	0.766	0.595	33.99%
RLS	RF	40.29%	0.727	0.565	31.17%
	OLS	27.76%	0.800	0.633	25.11%
OH	RF	46.29%	0.669	0.489	38.22%
	OLS	35.06%	0.736	0.557	34.68%
RH	RF	43.98%	0.666	0.522	35.46%
	OLS	33.44%	0.726	0.569	33.08%

675

676

677

678 **Figure:**



679

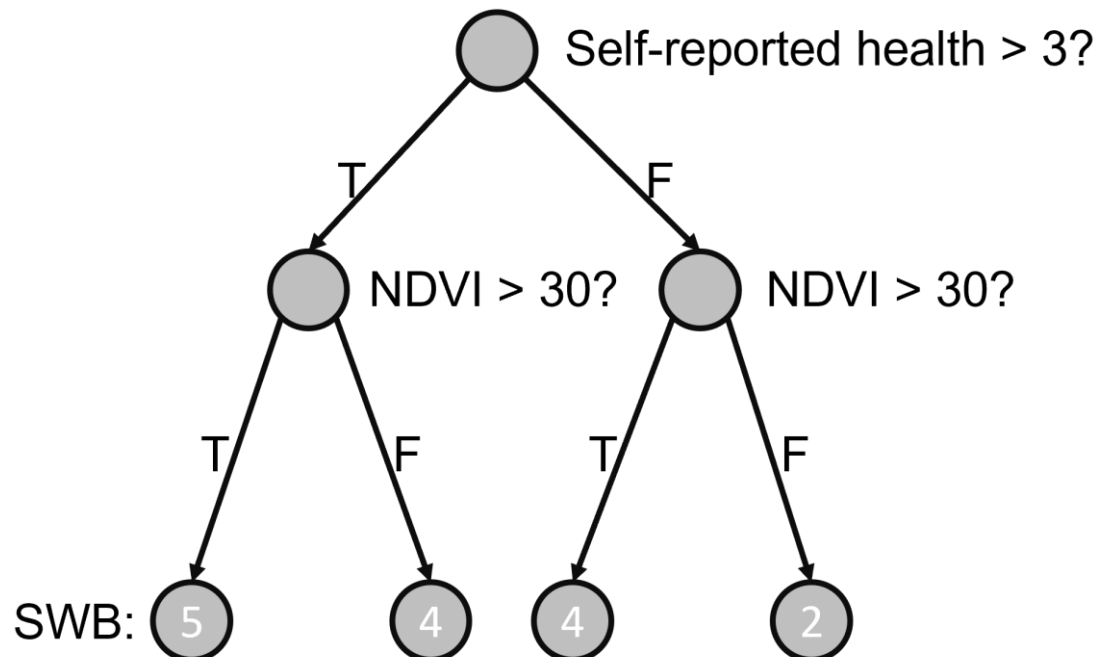
680

Figure 1: The Statistical Distributions of Critical Variables

681

(a: SWB; b: NDVI; c: NTL; d: Annual Income)

682

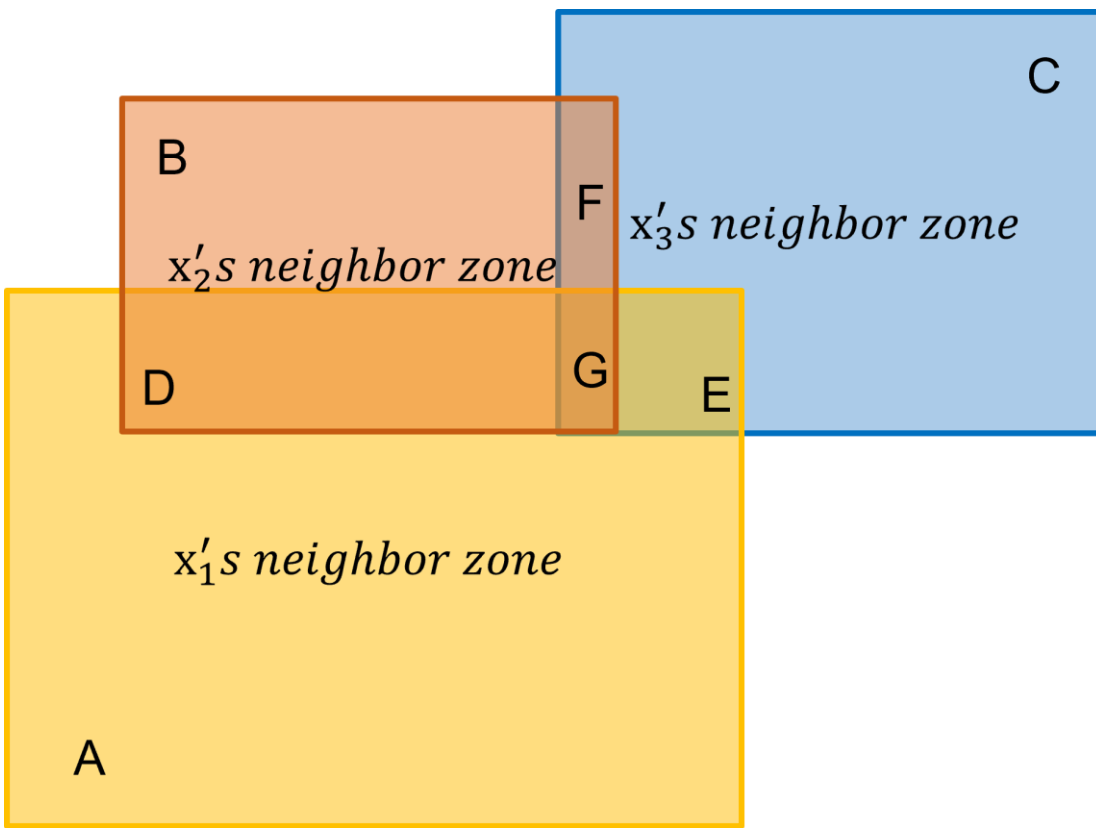


683

684

Figure 2: Example of a Regression Decision Tree

685

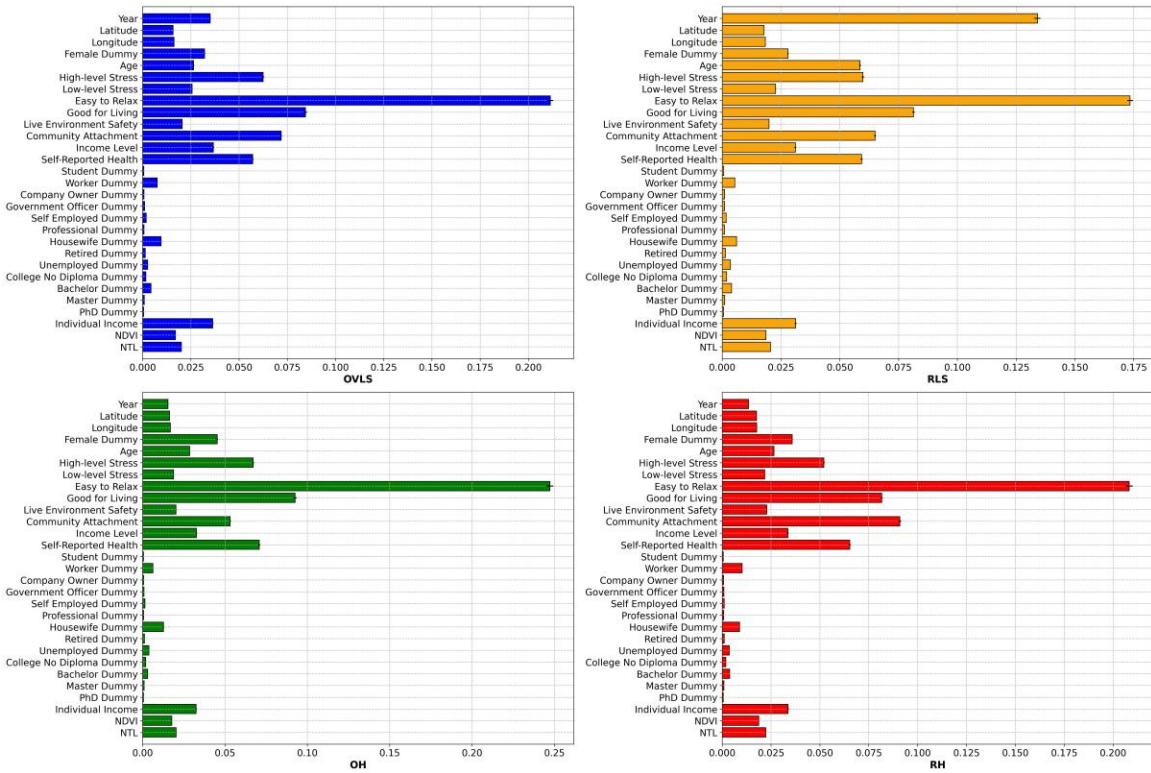


686

687

Figure 3: The Schematic Diagram of the Overlapped Neighbor Zones

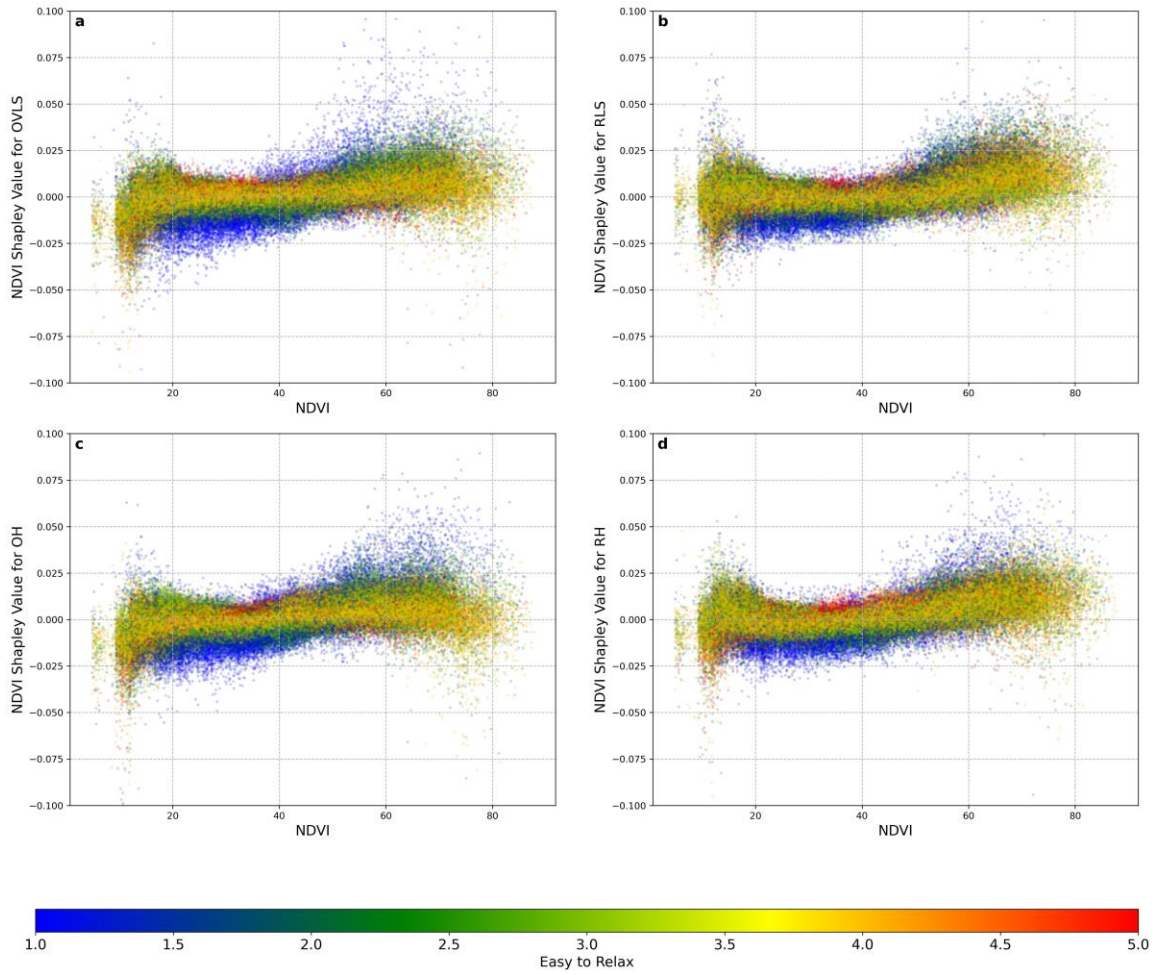
688



689

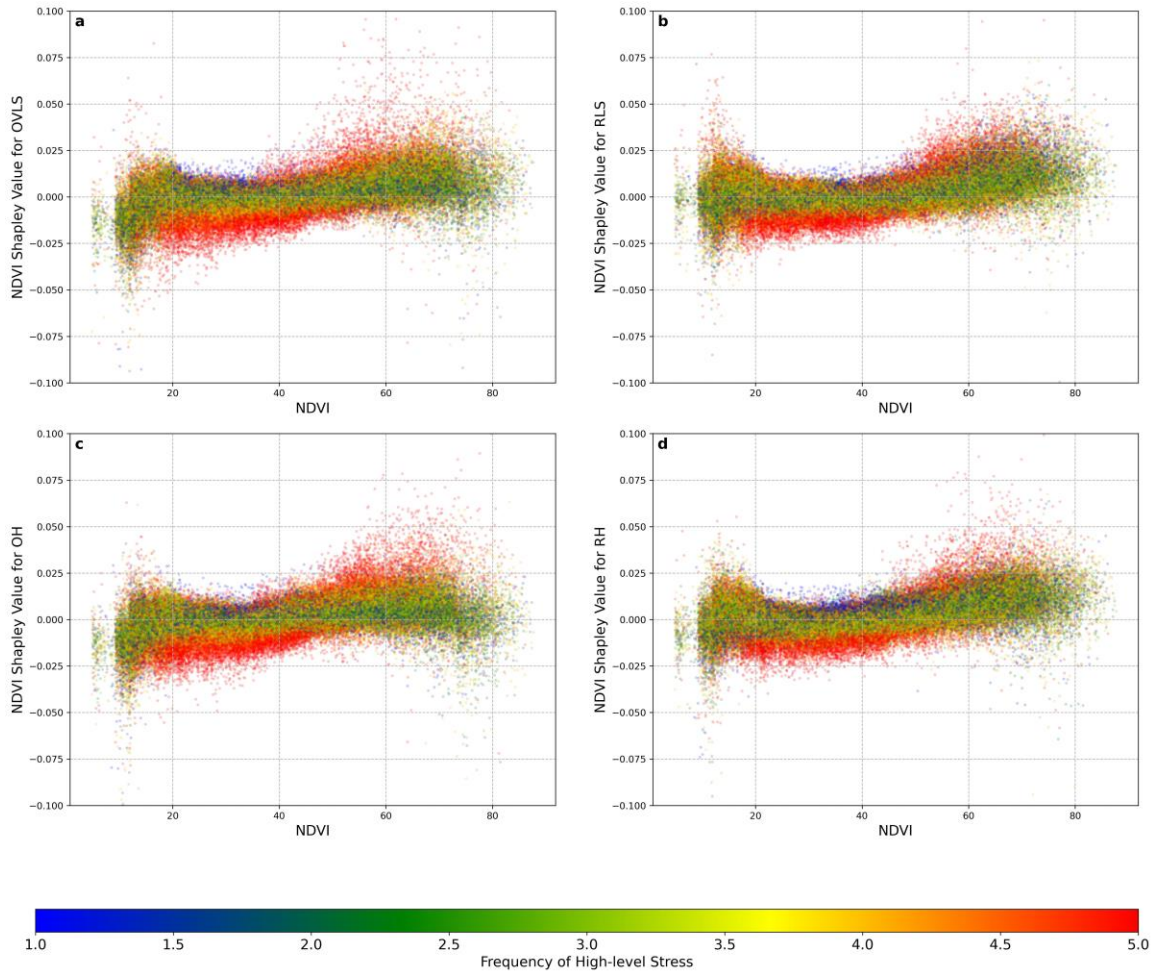
690

Figure 4: The Importance of Features



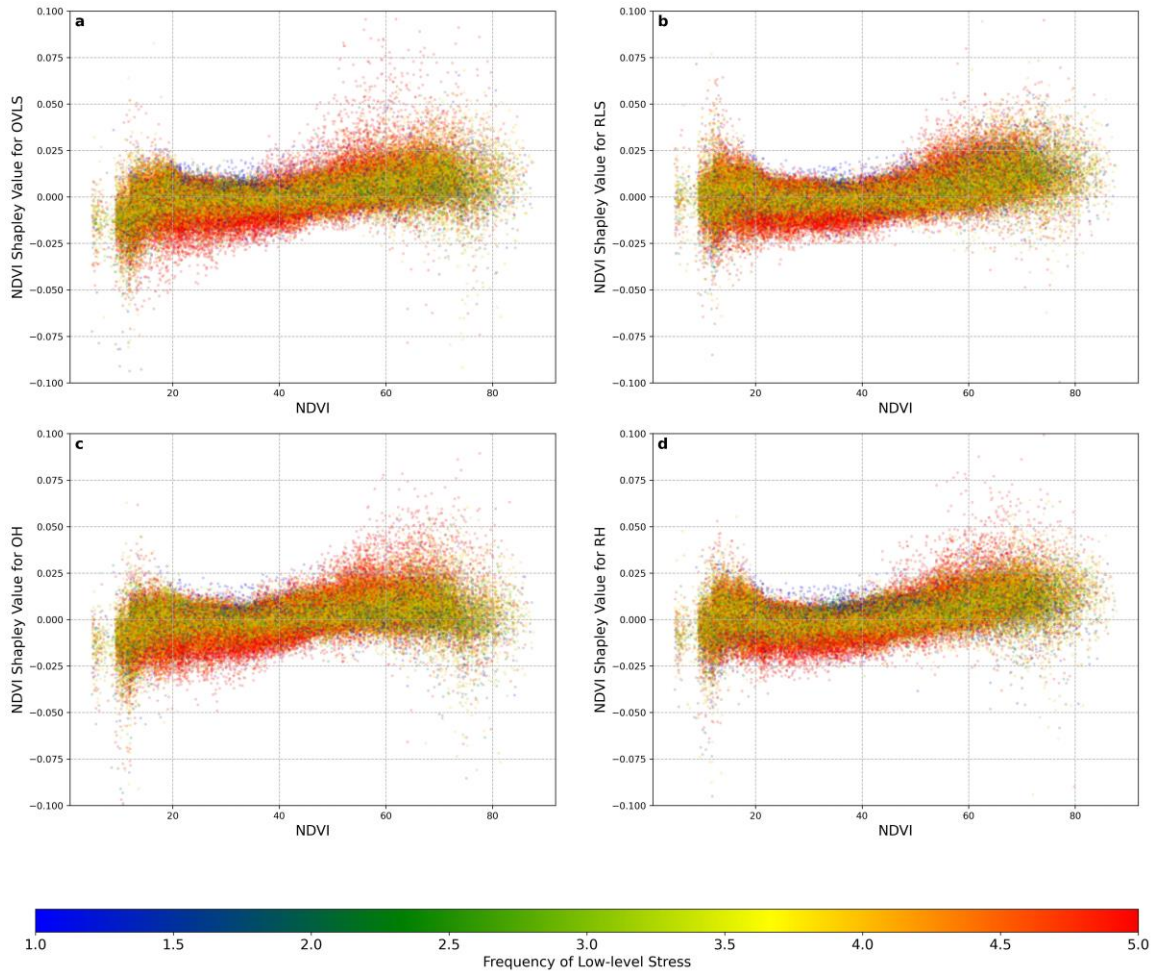
691

692 **Figure 5: The Scatter Plot between NDVI and Its Contributions to SWB Colored by
693 Value of Feature, Easy to Relax**



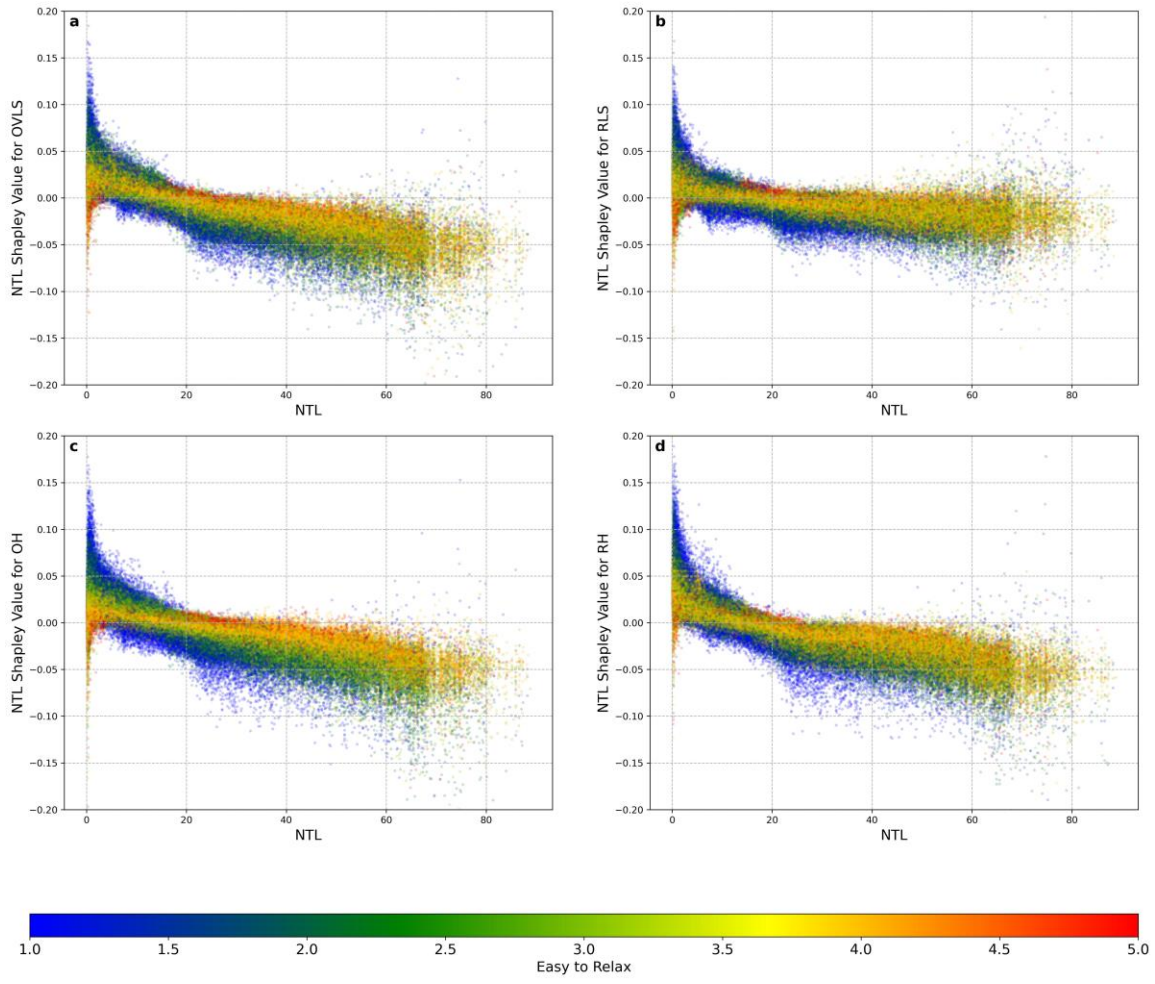
694

695 **Figure 6: The Scatter Plot between NDVI and Its Contributions to SWB Colored by**
 696 **Value of Feature, Frequency of High-level Stress**



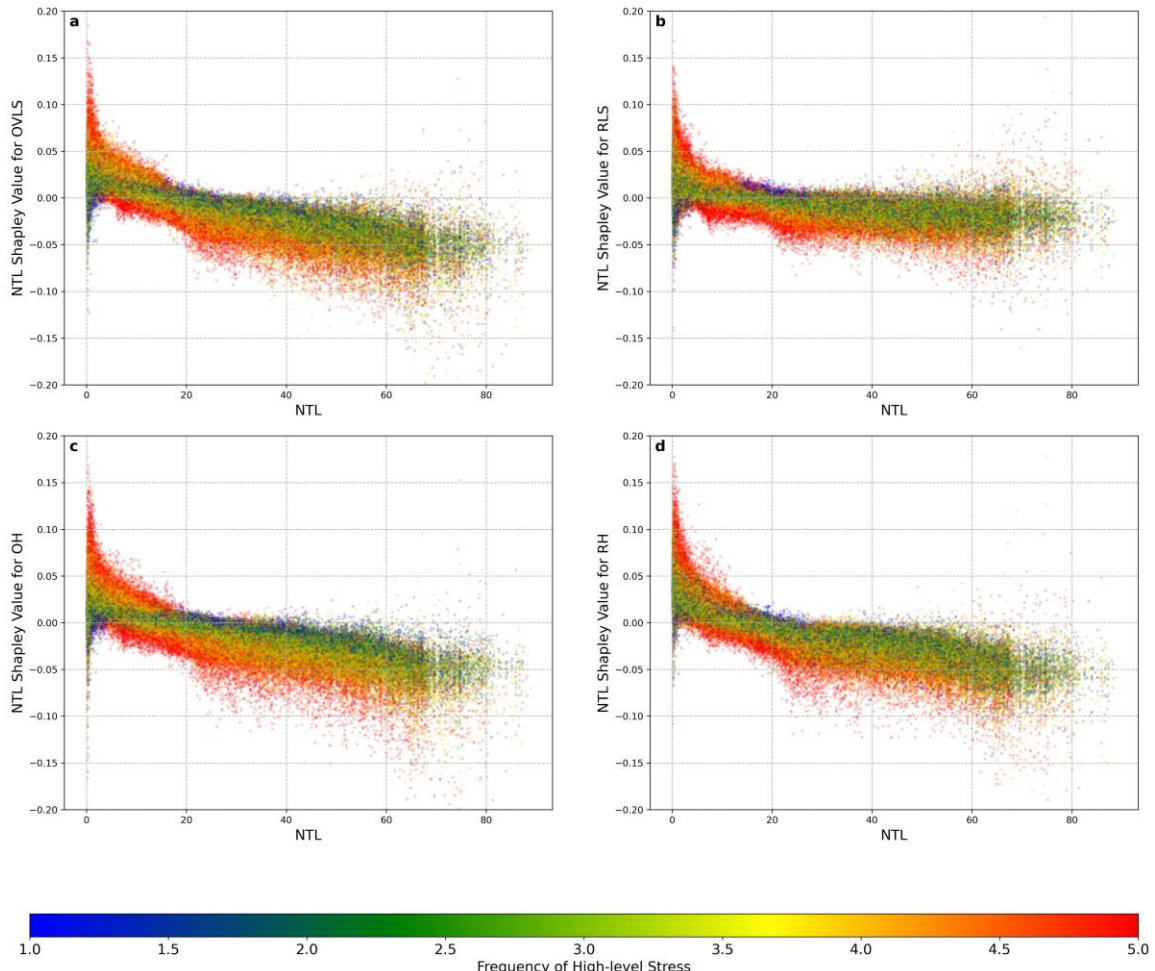
697

698 **Figure 7: The Scatter Plot between NDVI and Its Contributions to SWB Colored by**
 699 **Value of Feature, Frequency of Low-level Stress**



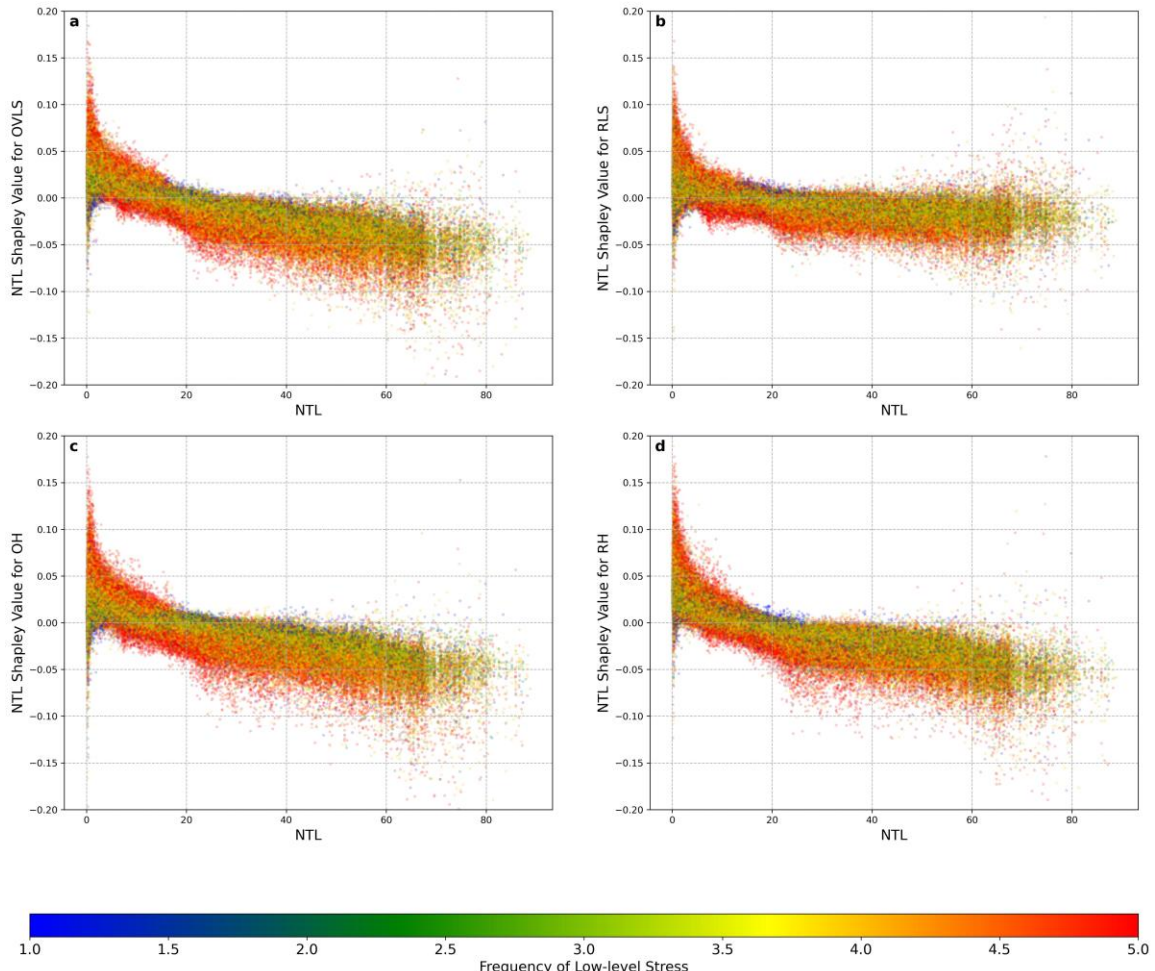
700

701 **Figure 8: The Scatter Plot between NTL and Its Contributions to SWB Colored by**
 702 **Value of Feature, Easy to Relax**



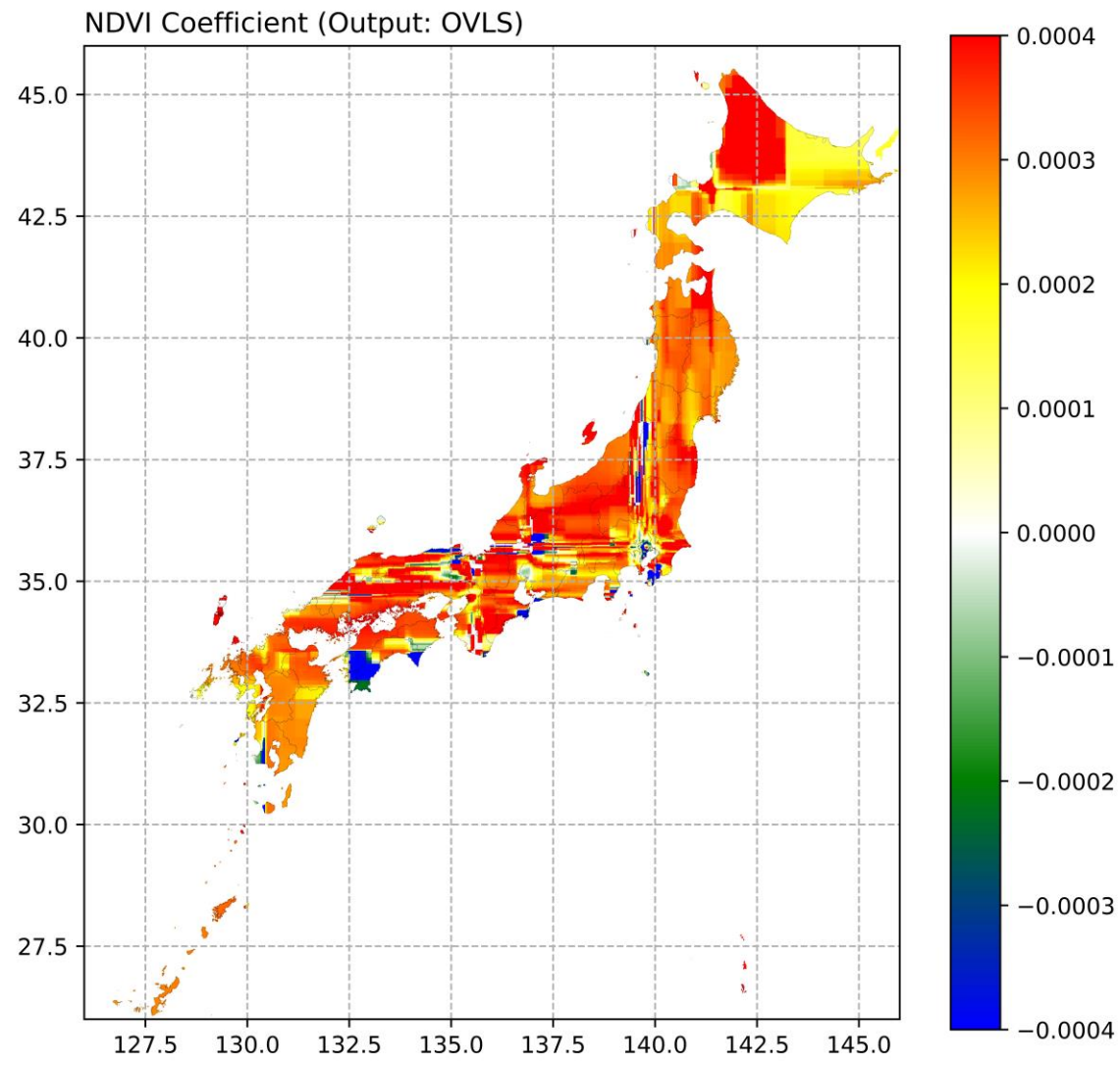
703

704 **Figure 9: The Scatter Plot between NTL and Its Contributions to SWB Colored by
705 Value of Feature, Frequency of High-level Stress**



706

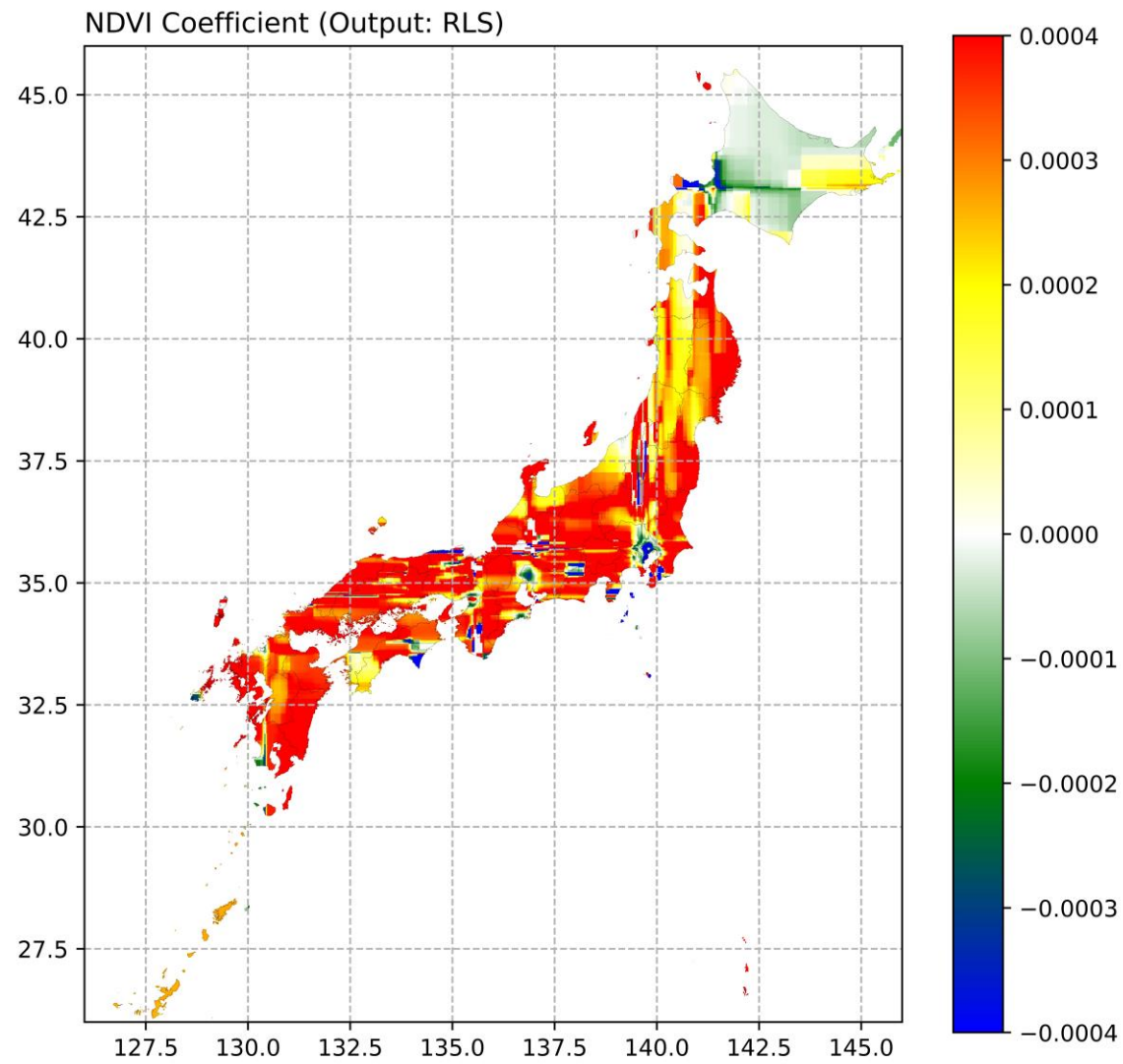
707 **Figure 10: The Scatter Plot between NTL and Its Contributions to SWB Colored by
 708 Value of Feature, Frequency of Low-level Stress**



709

710

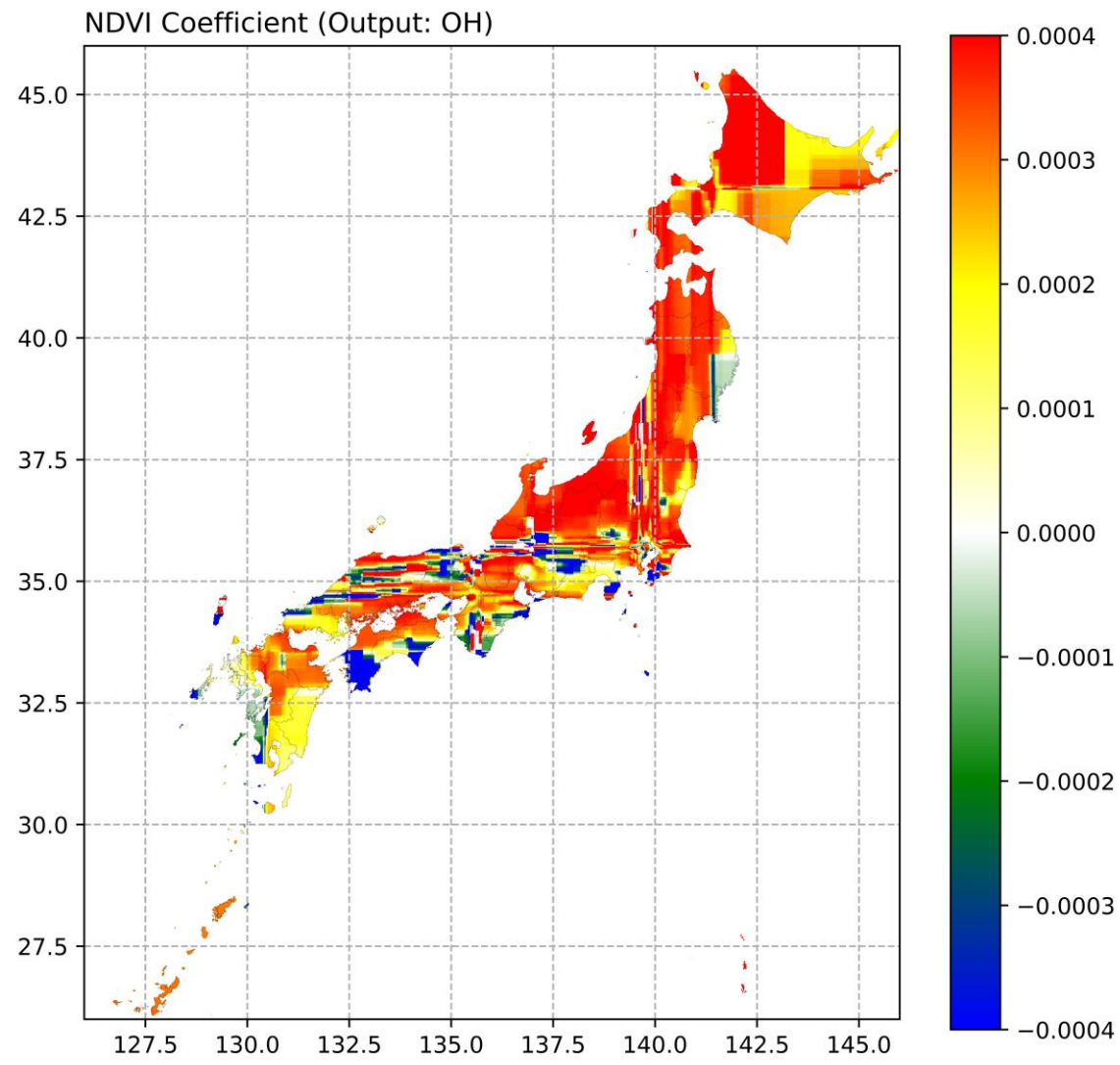
Figure 11: The Geographically Average Effect of NDVI on OVLS



711

712

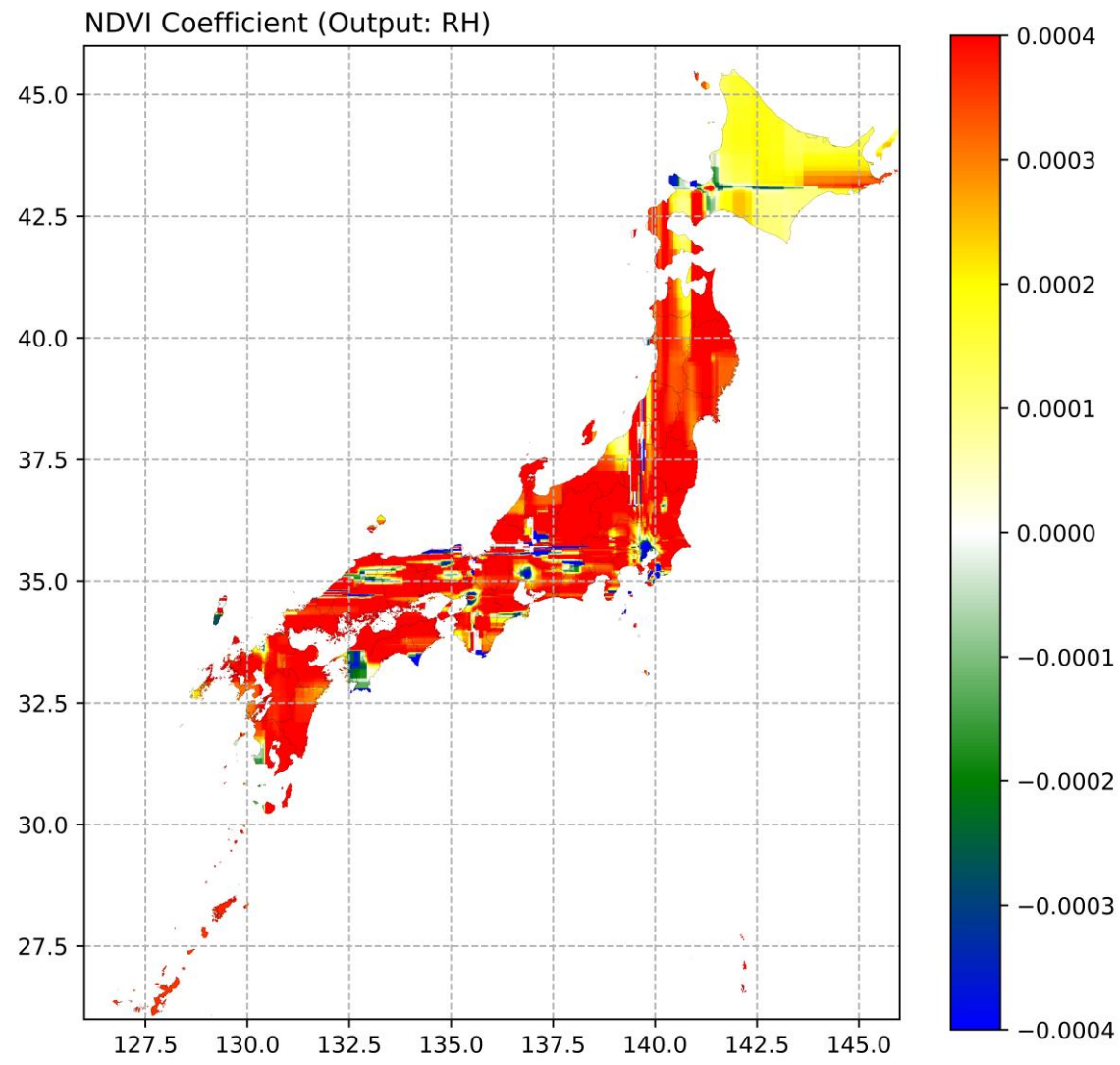
Figure 12: The Geographically Average Effect of NDVI on RLS



713

714

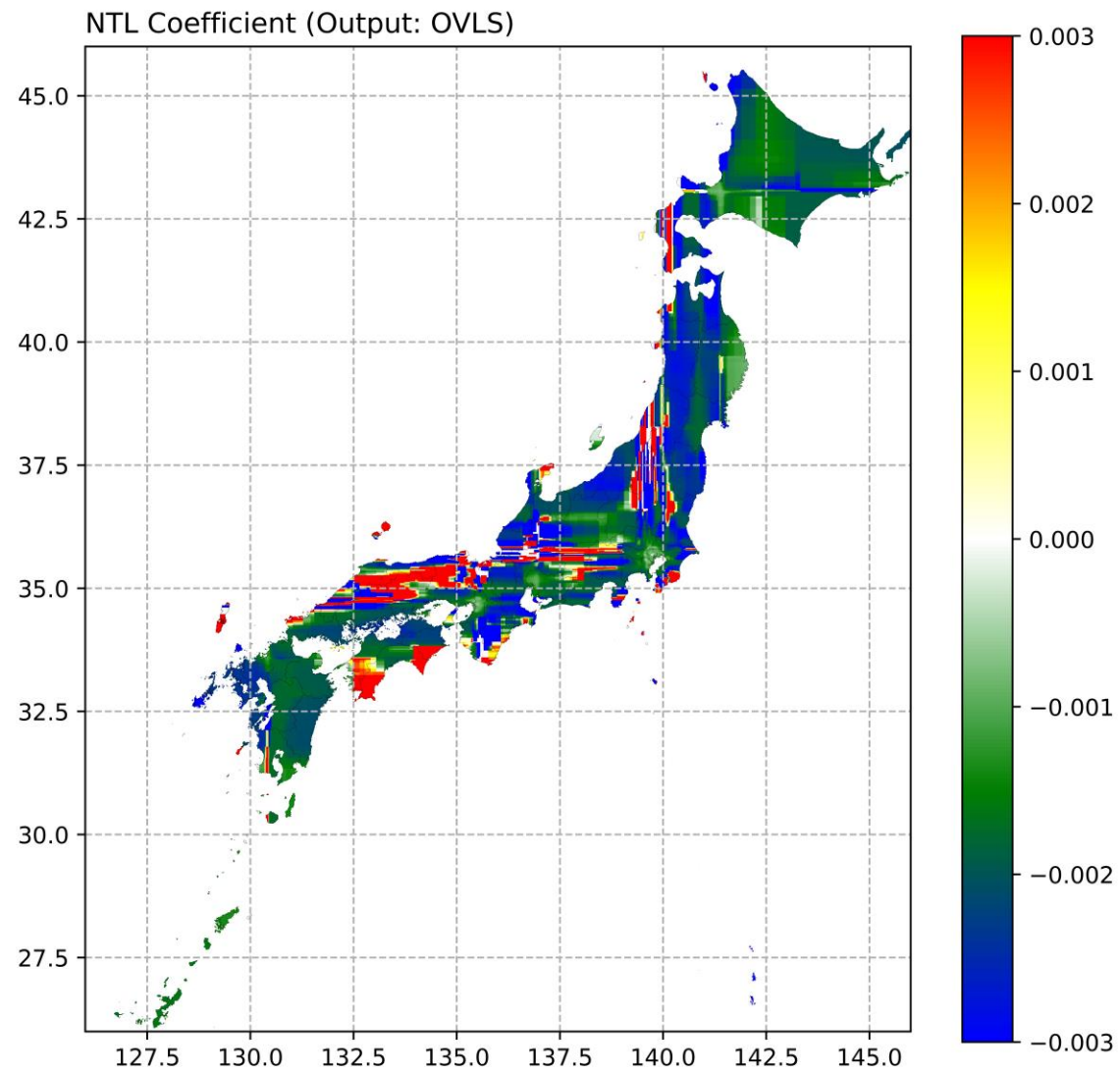
Figure 13: The Geographically Average Effect of NDVI on OH



715

716

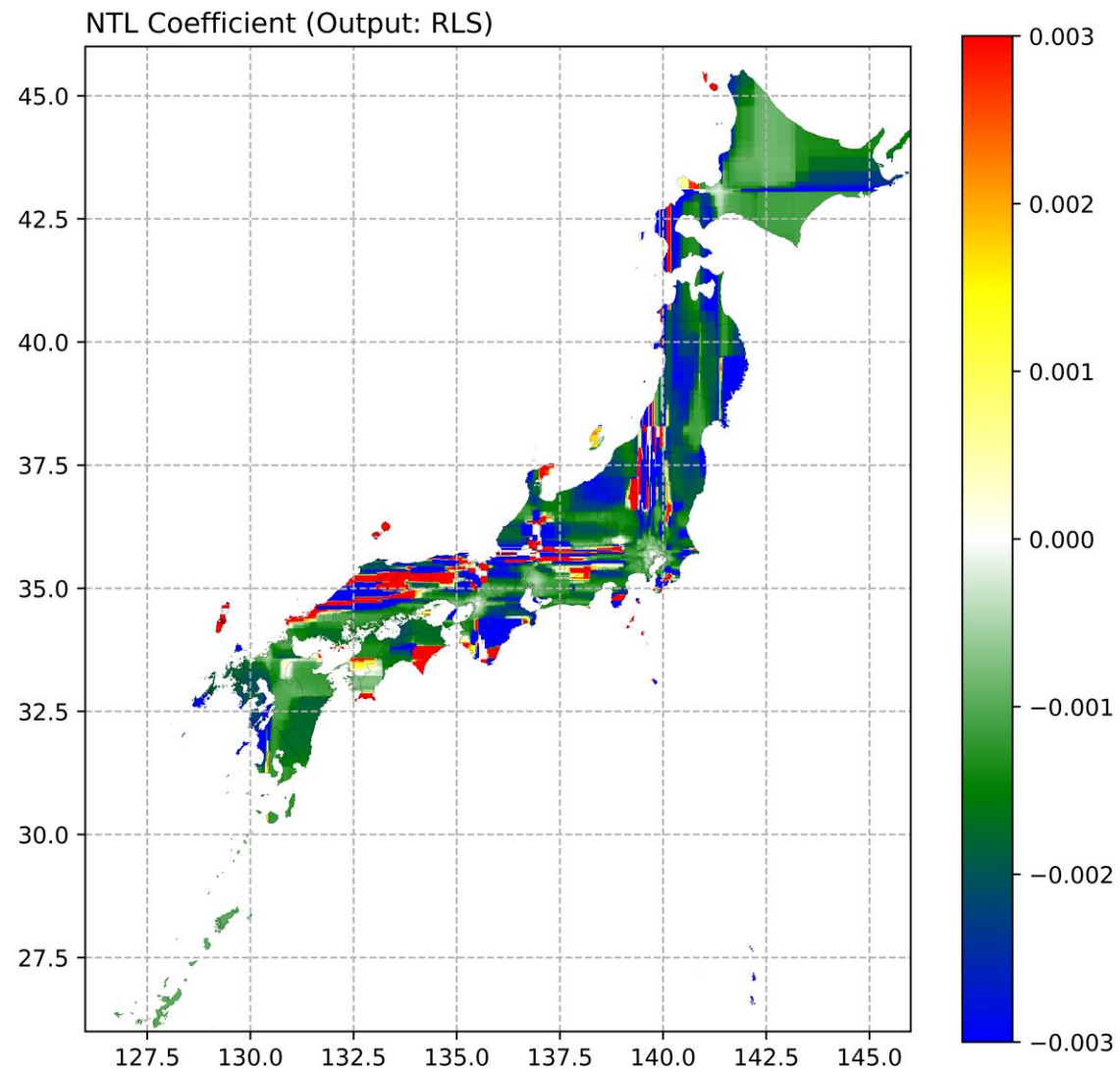
Figure 14: The Geographically Average Effect of NDVI on RH



717

718

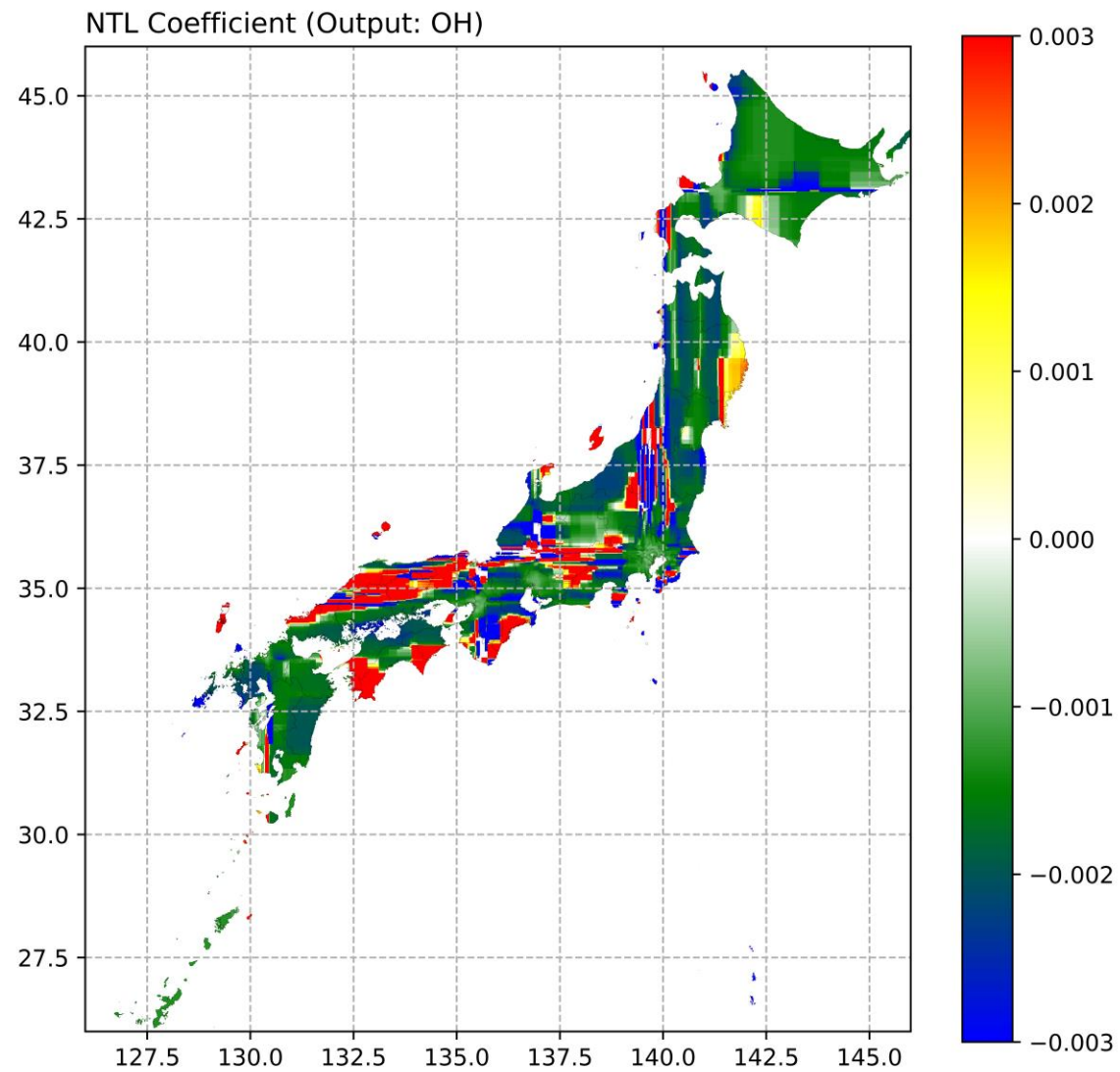
Figure 15: The Geographically Average Effect of NTL on OVLS



719

720

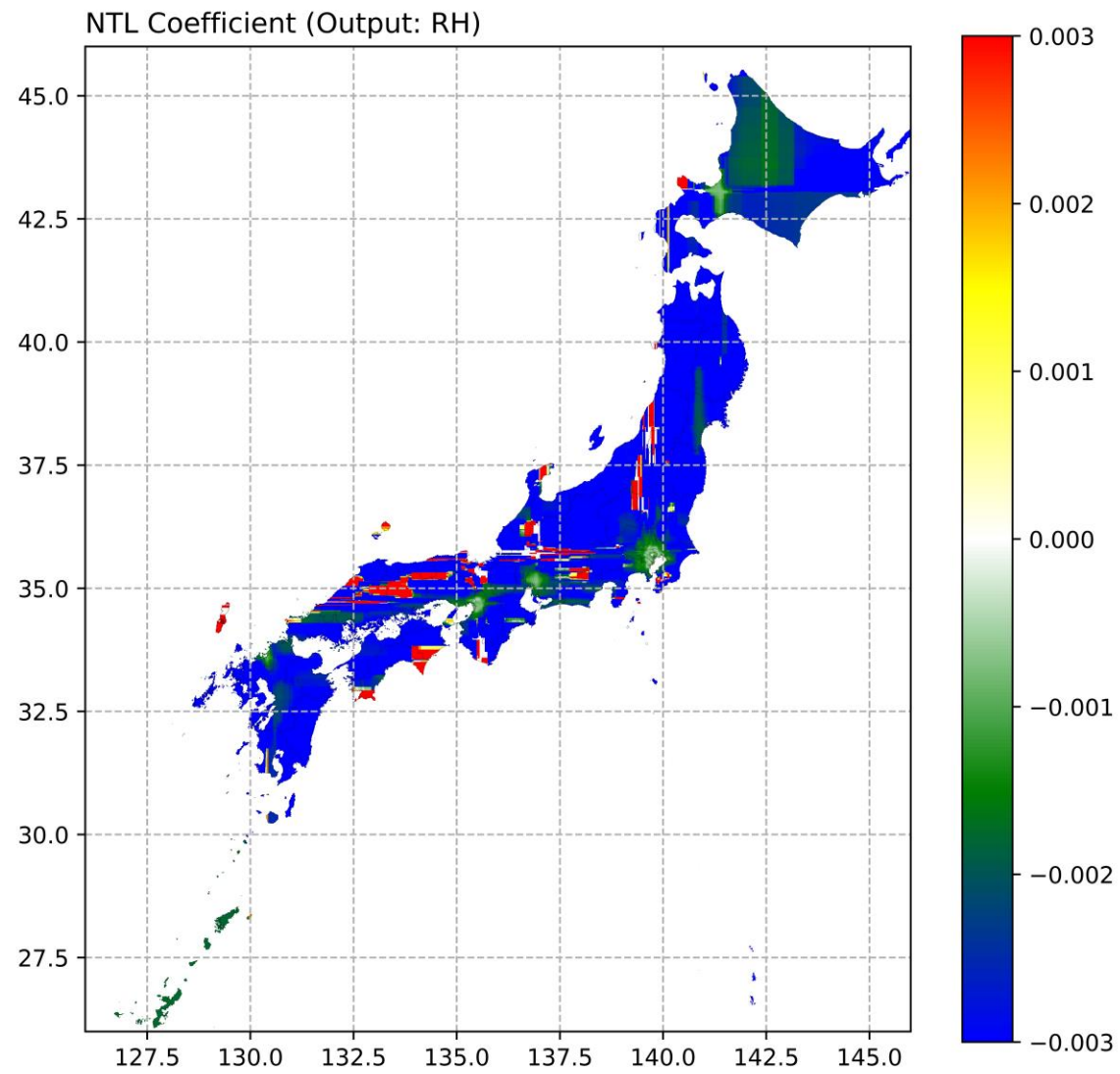
Figure 16: The Geographically Average Effect of NTL on RLS



721

722

Figure 17: The Geographically Average Effect of NTL on OH

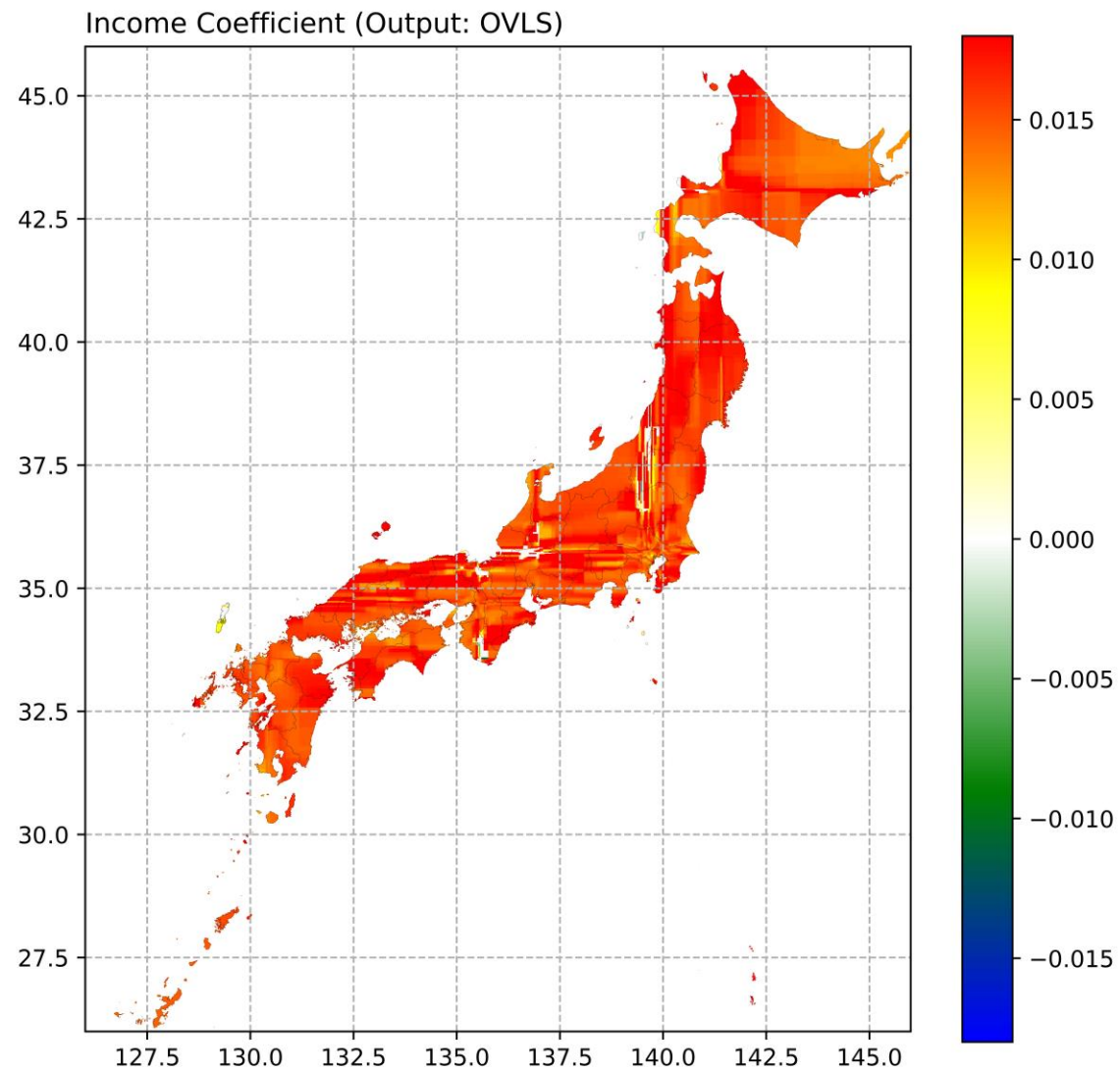


723

724

Figure 18: The Geographically Average Effect of NTL on RH

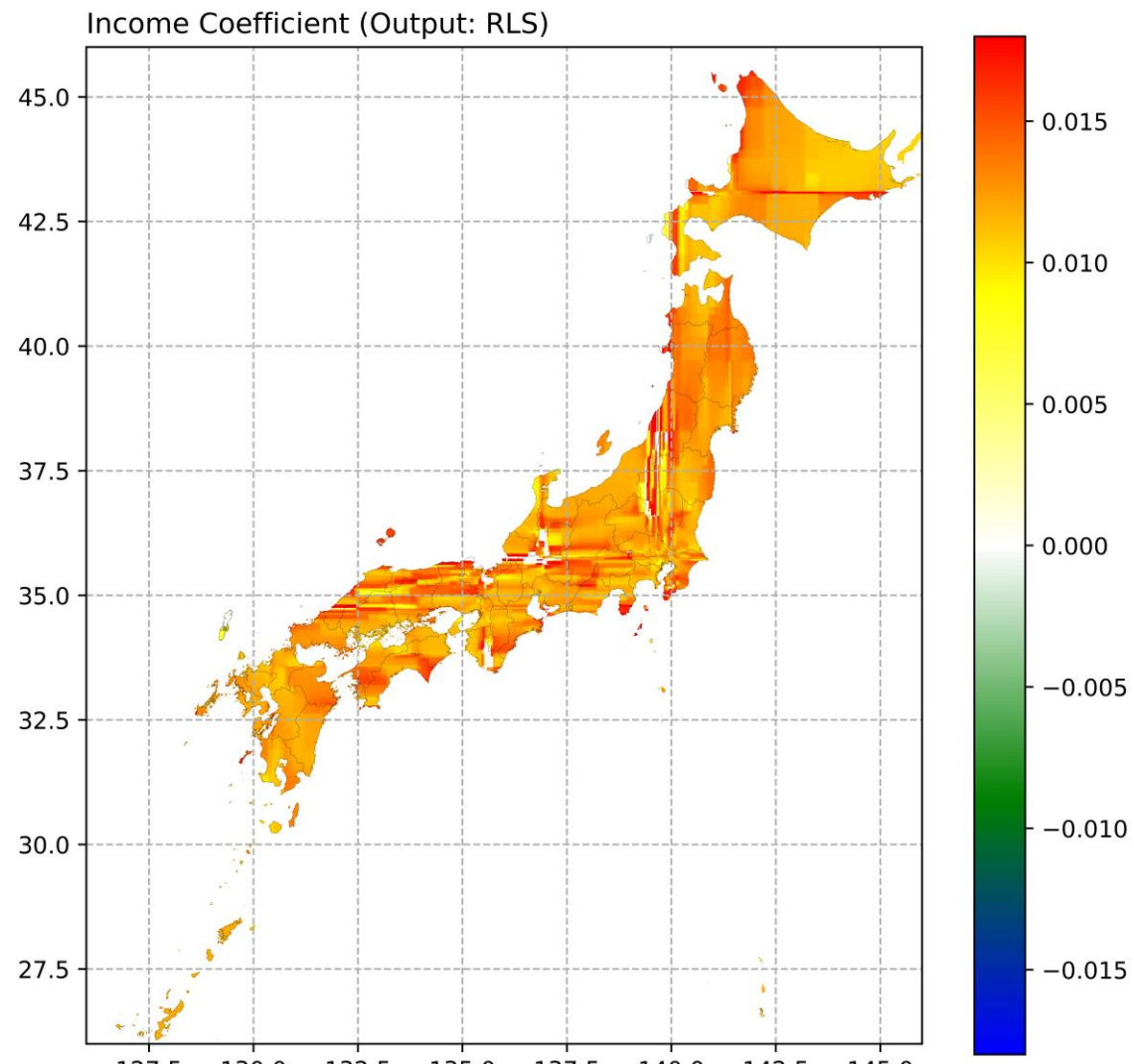
725



726

Figure 19: The Geographically Average Effect of Income on OVLS

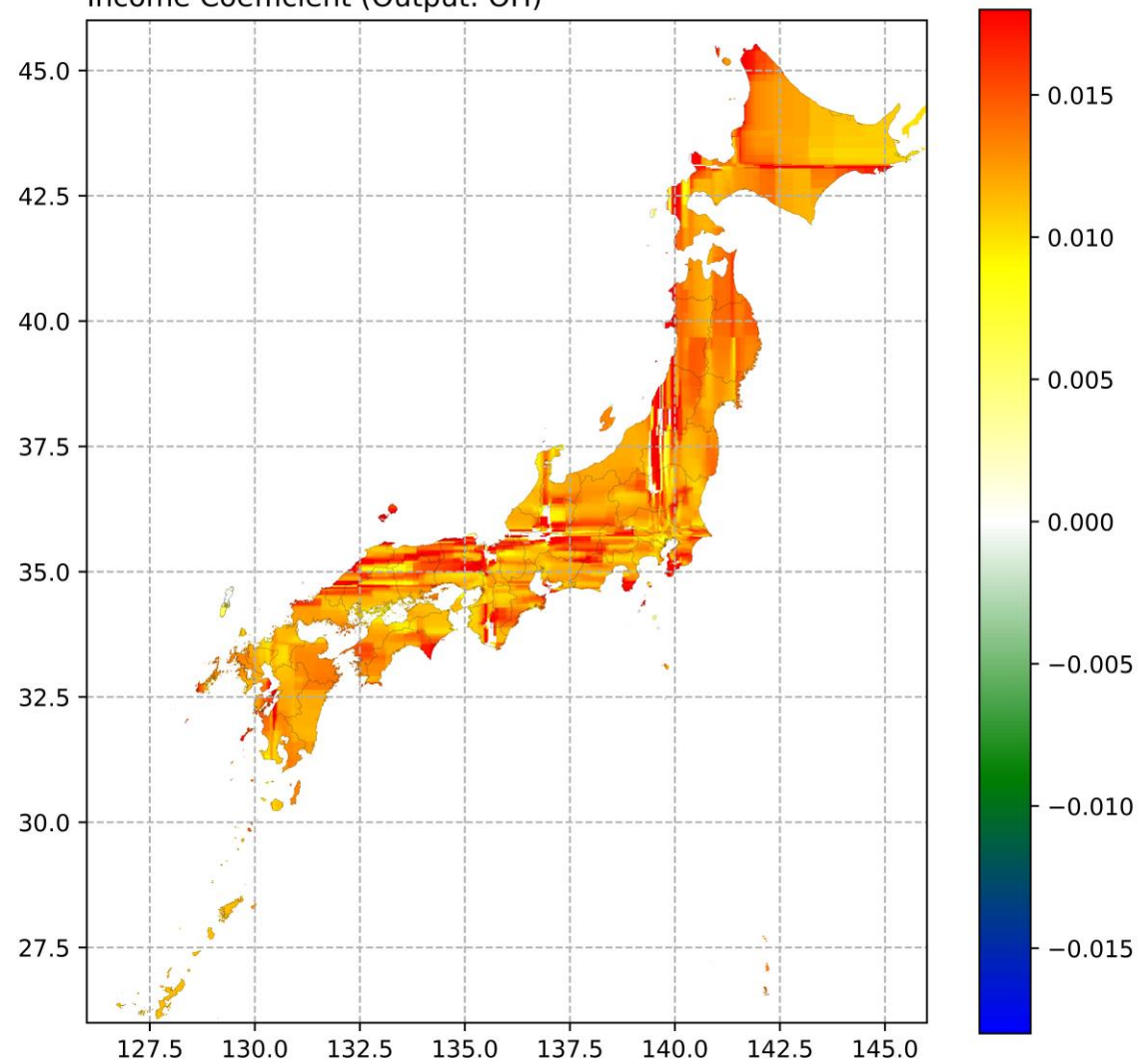
727



728

Figure 20: The Geographically Average Effect of Income on RLS

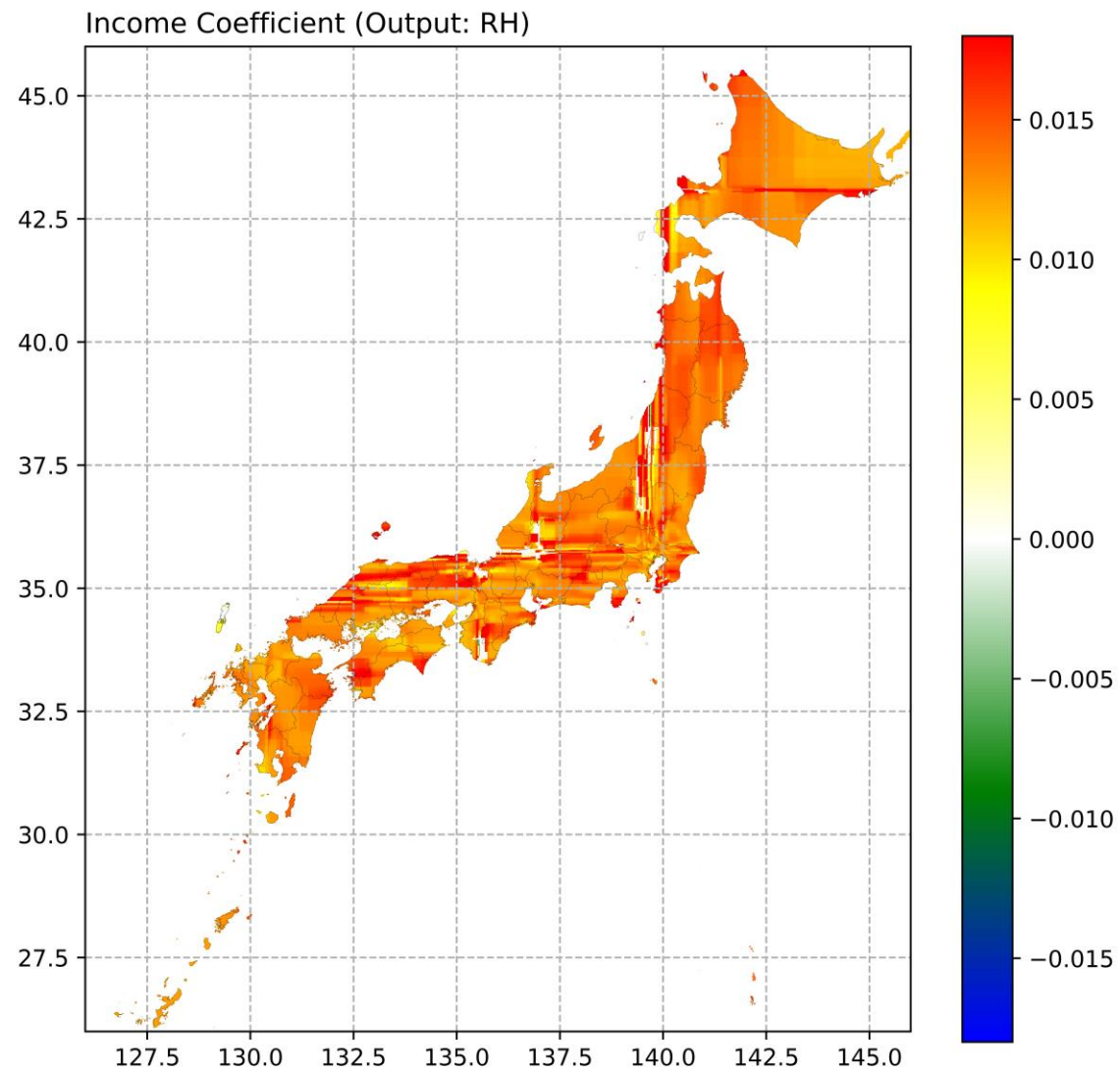
Income Coefficient (Output: OH)



729

730

Figure 21: The Geographically Average Effect of Income on OH

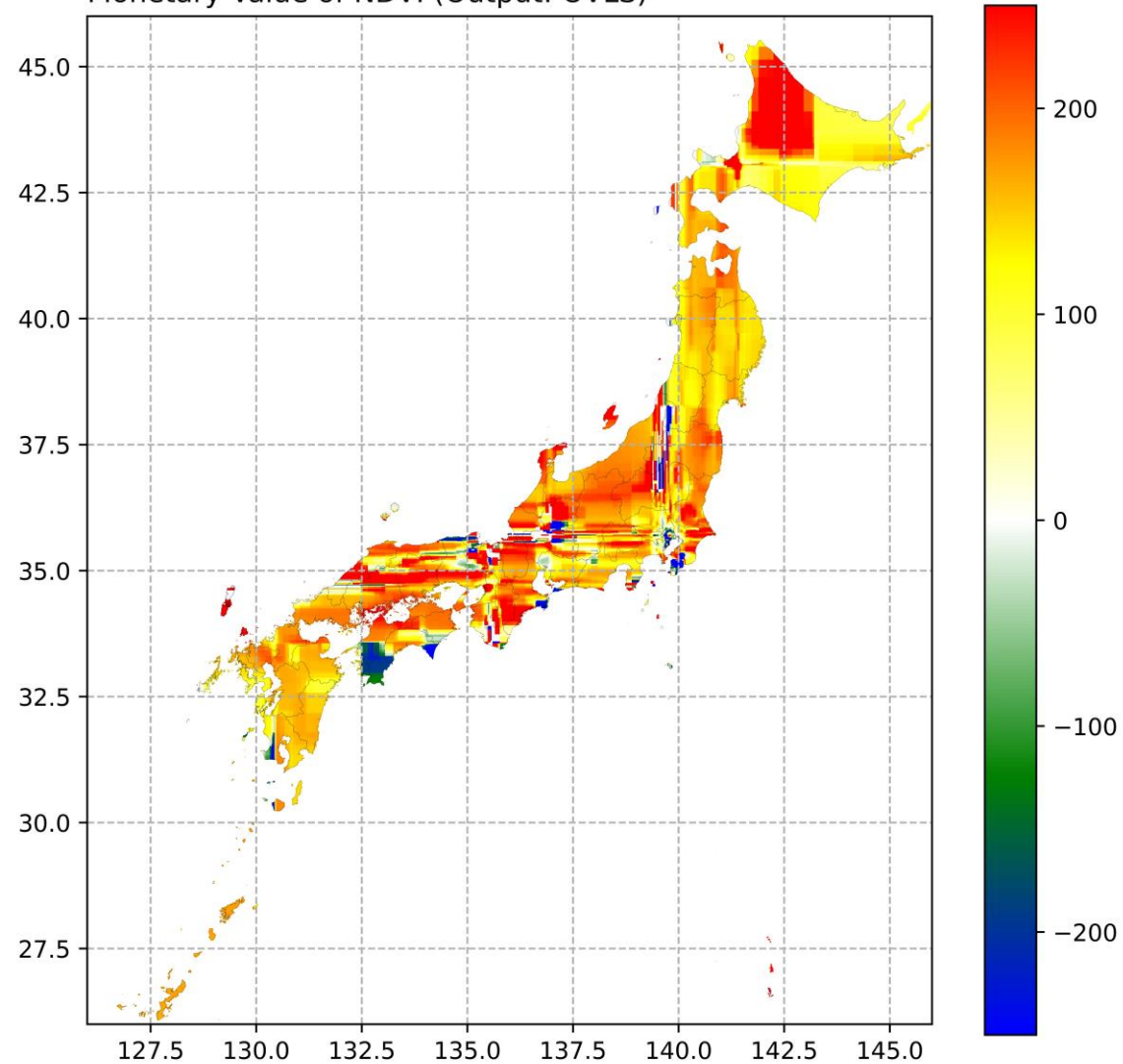


731

732

Figure 22: The Geographically Average Effect of Income on RH

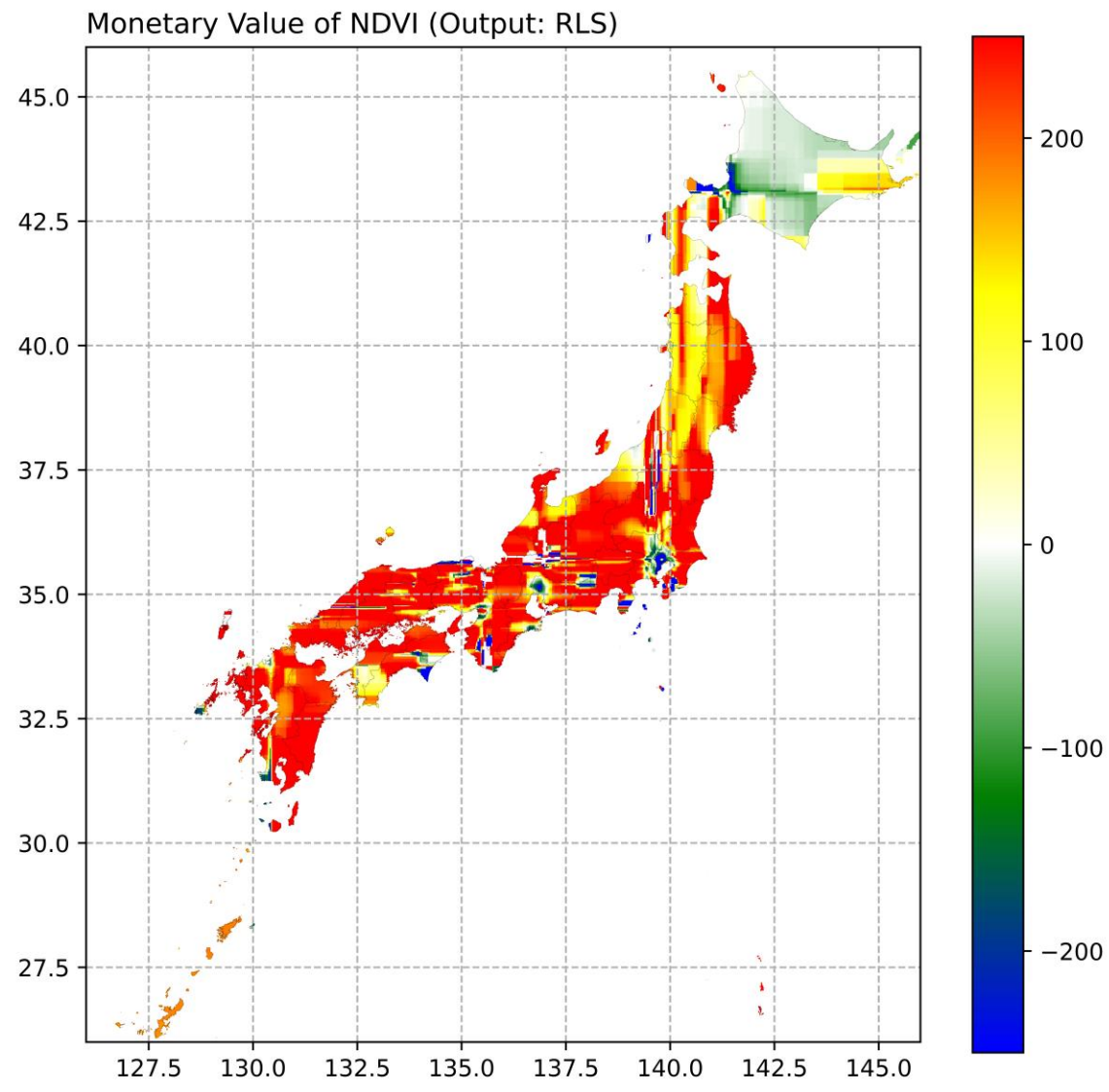
Monetary Value of NDVI (Output: OVLS)



733

734

Figure 23: The Monetary Value of NDVI on OVLS (unit: USD/%)

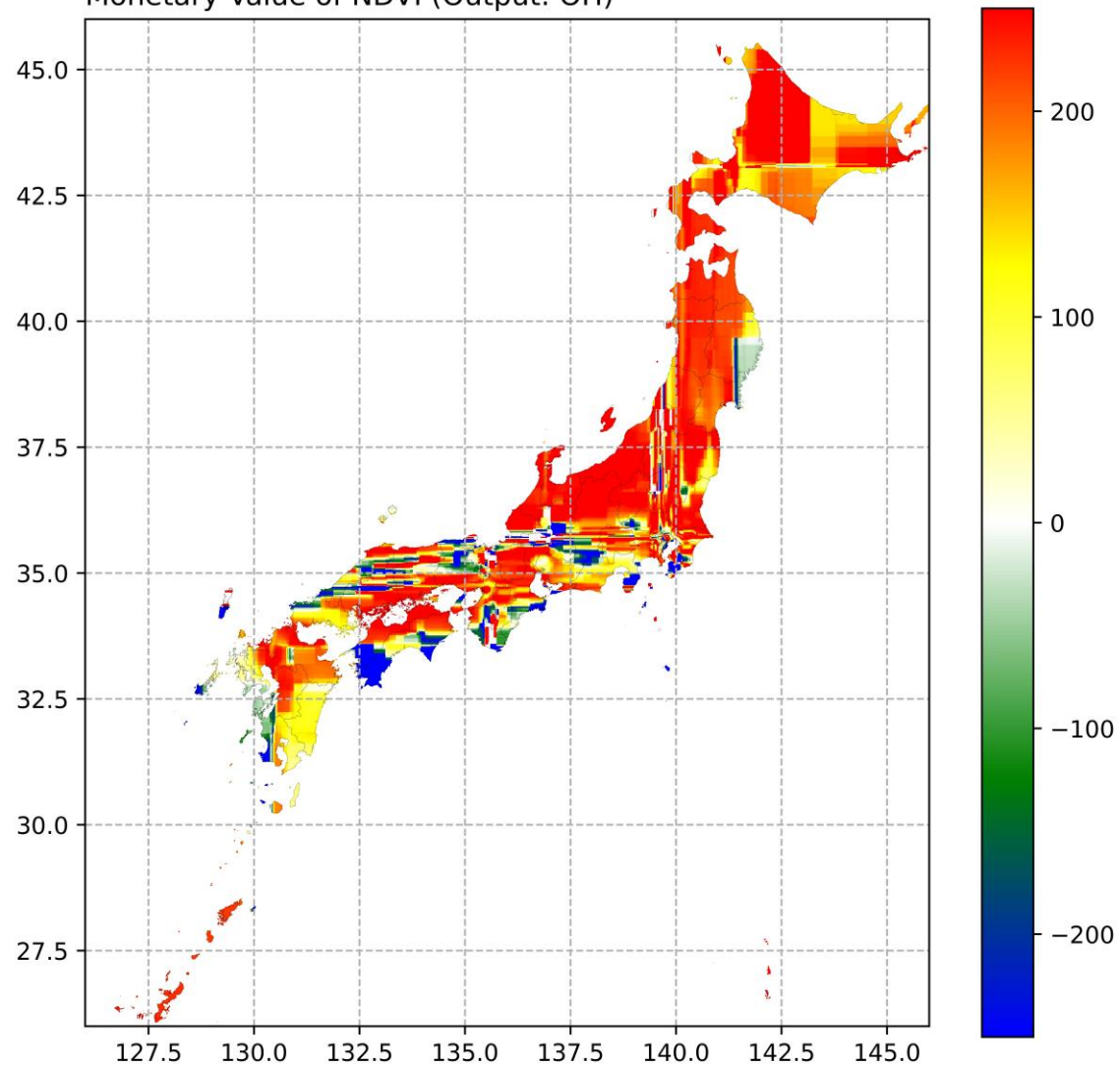


735

736

Figure 24: The Monetary Value of NDVI on RLS (unit: USD/%)

Monetary Value of NDVI (Output: OH)

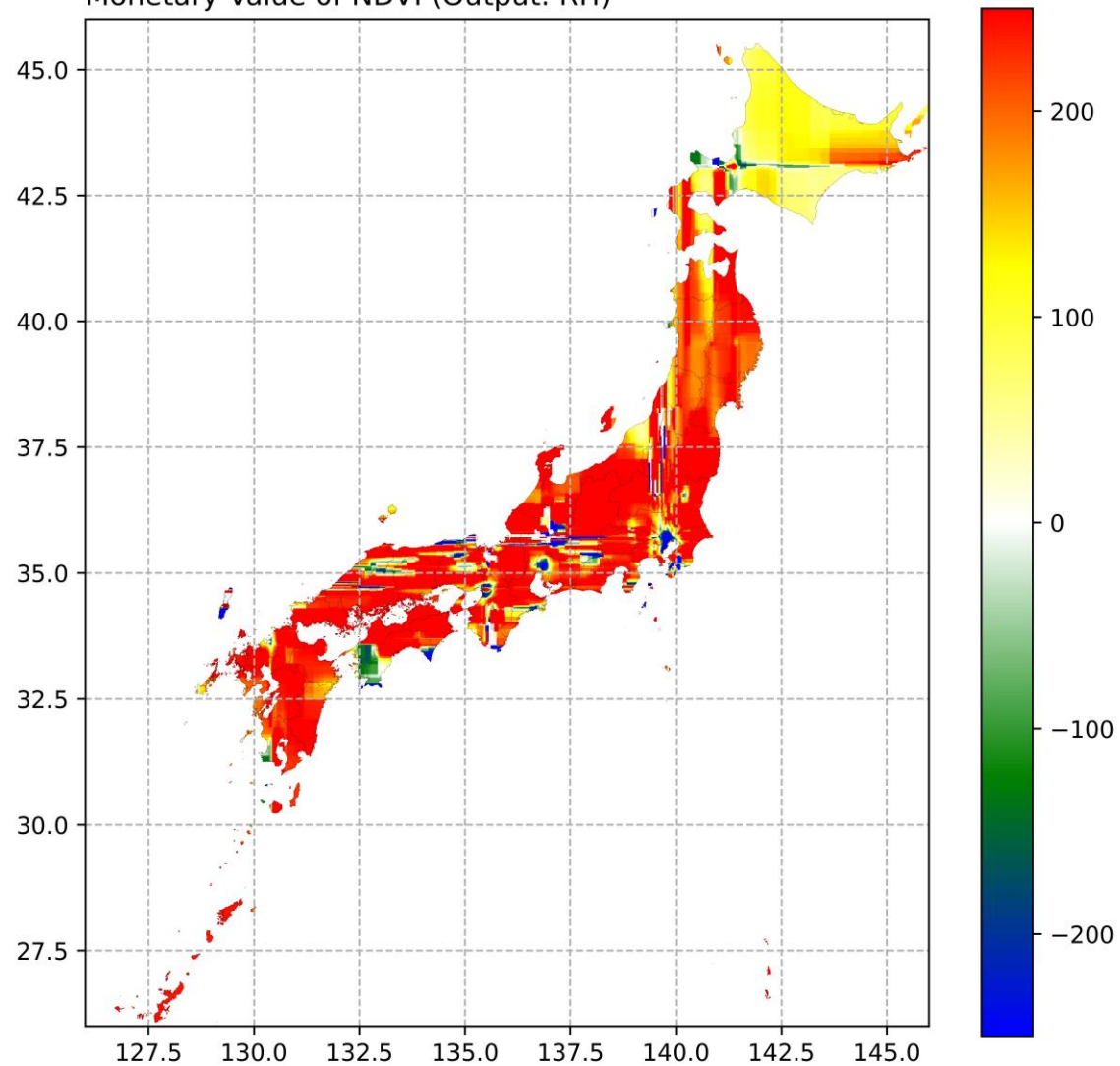


737

738

Figure 25: The Monetary Value of NDVI on OH (unit: USD/%)

Monetary Value of NDVI (Output: RH)

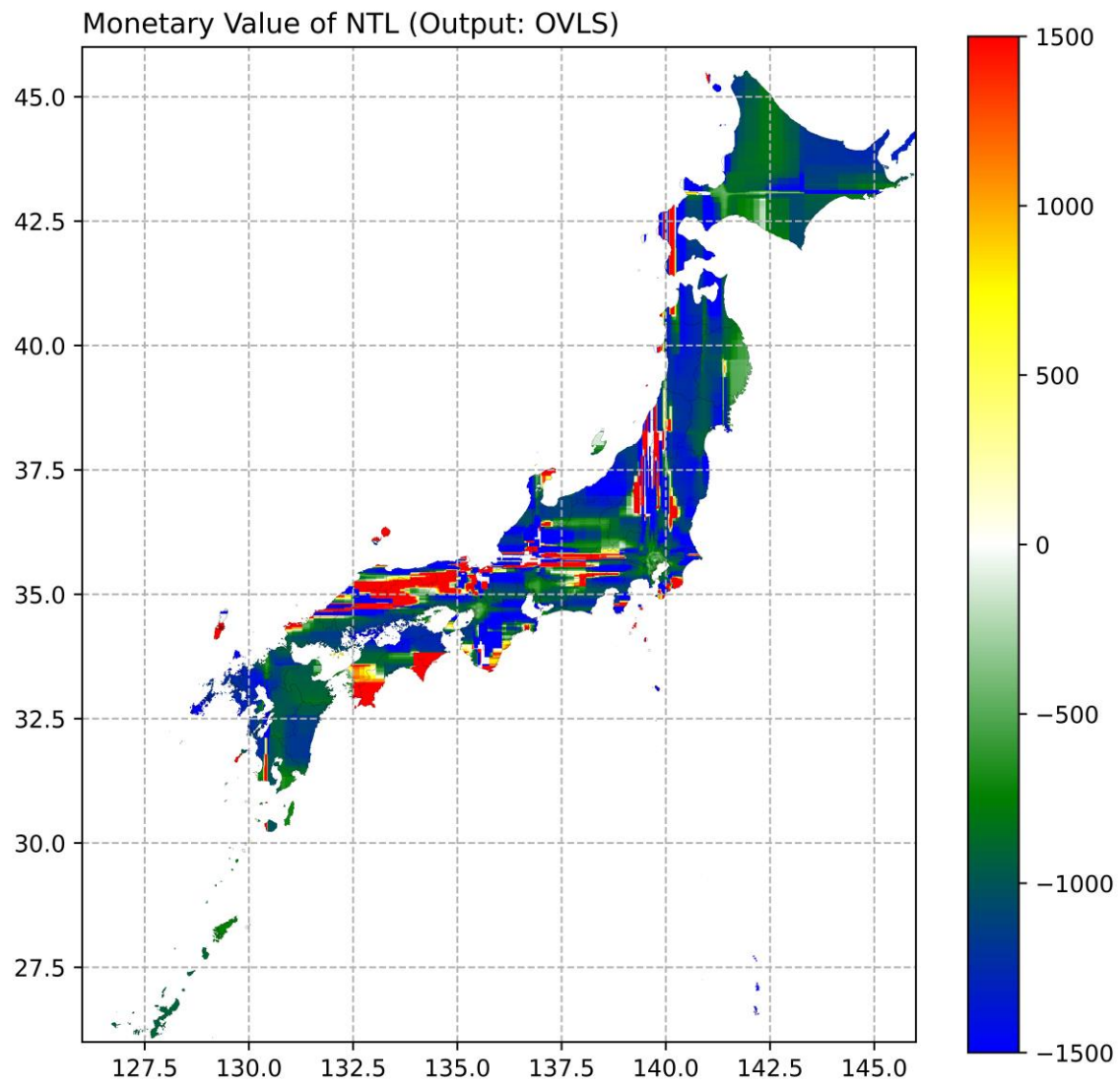


739

740

Figure 26: The Monetary Value of NDVI on RH (unit: USD/%)

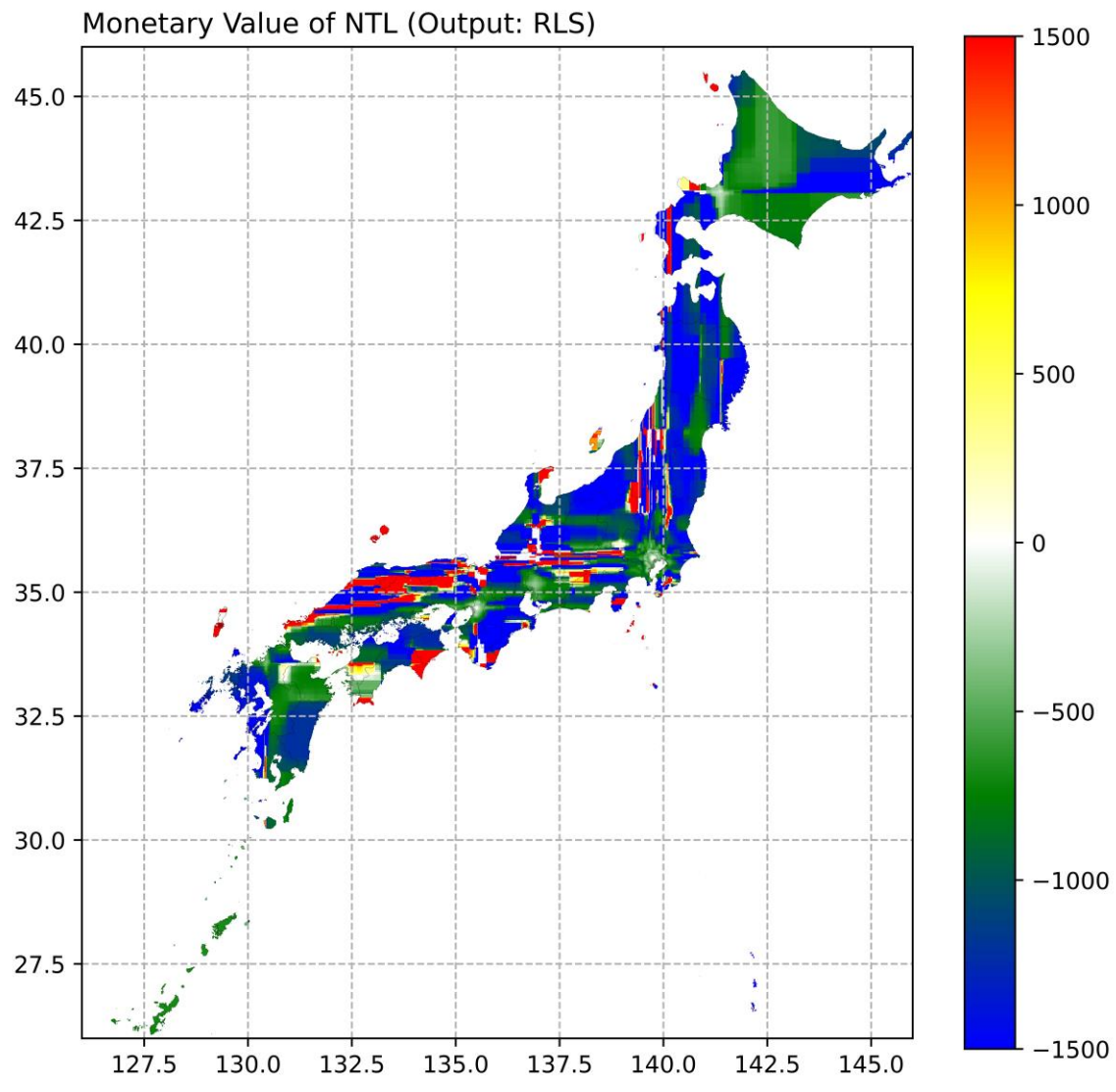
741



742

Figure 27: The Monetary Value of NDVI on OVLS (unit: $\text{USD}/(\text{nW}/\text{cm}^2 \cdot \text{sr})$)

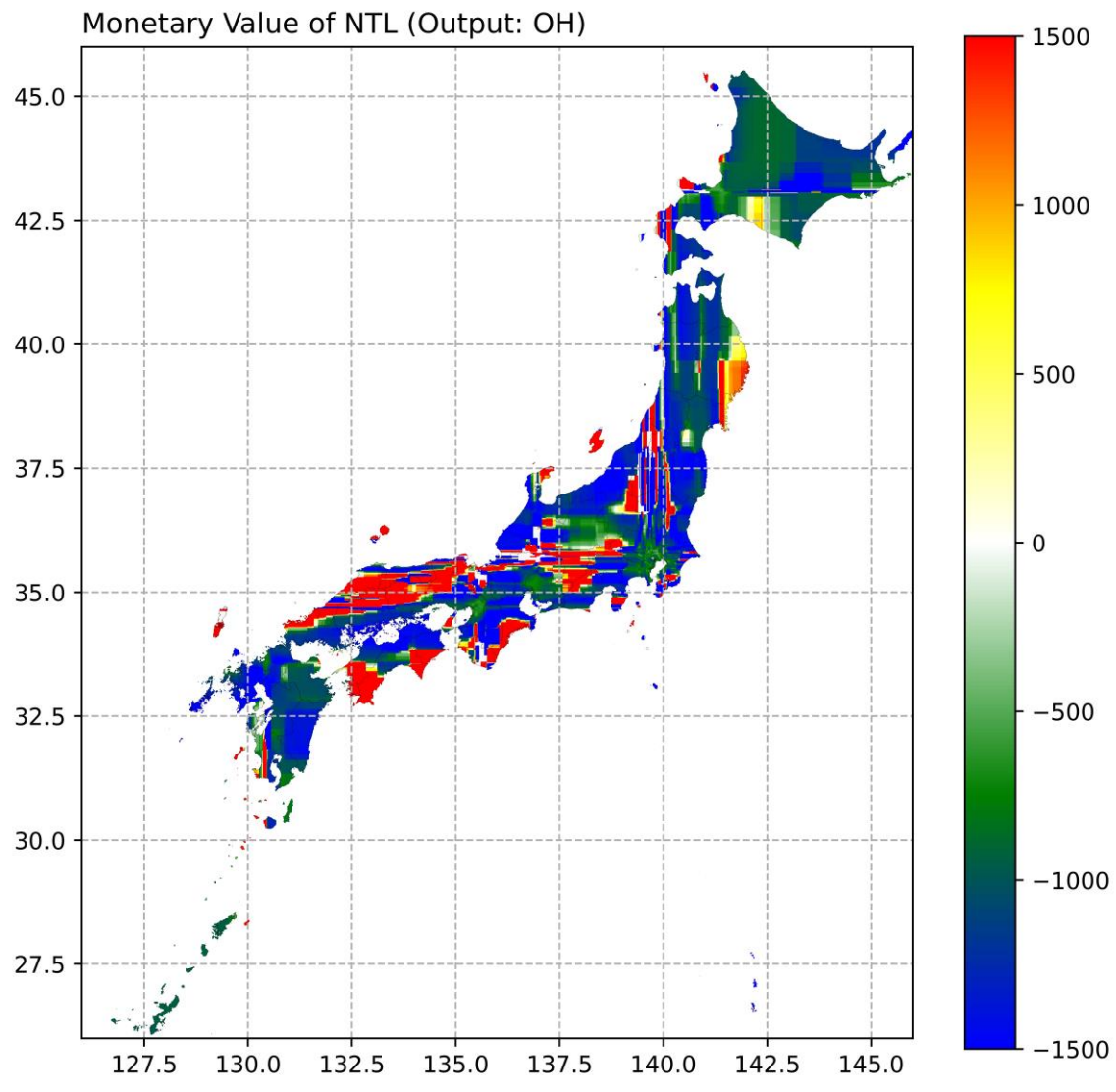
743



744

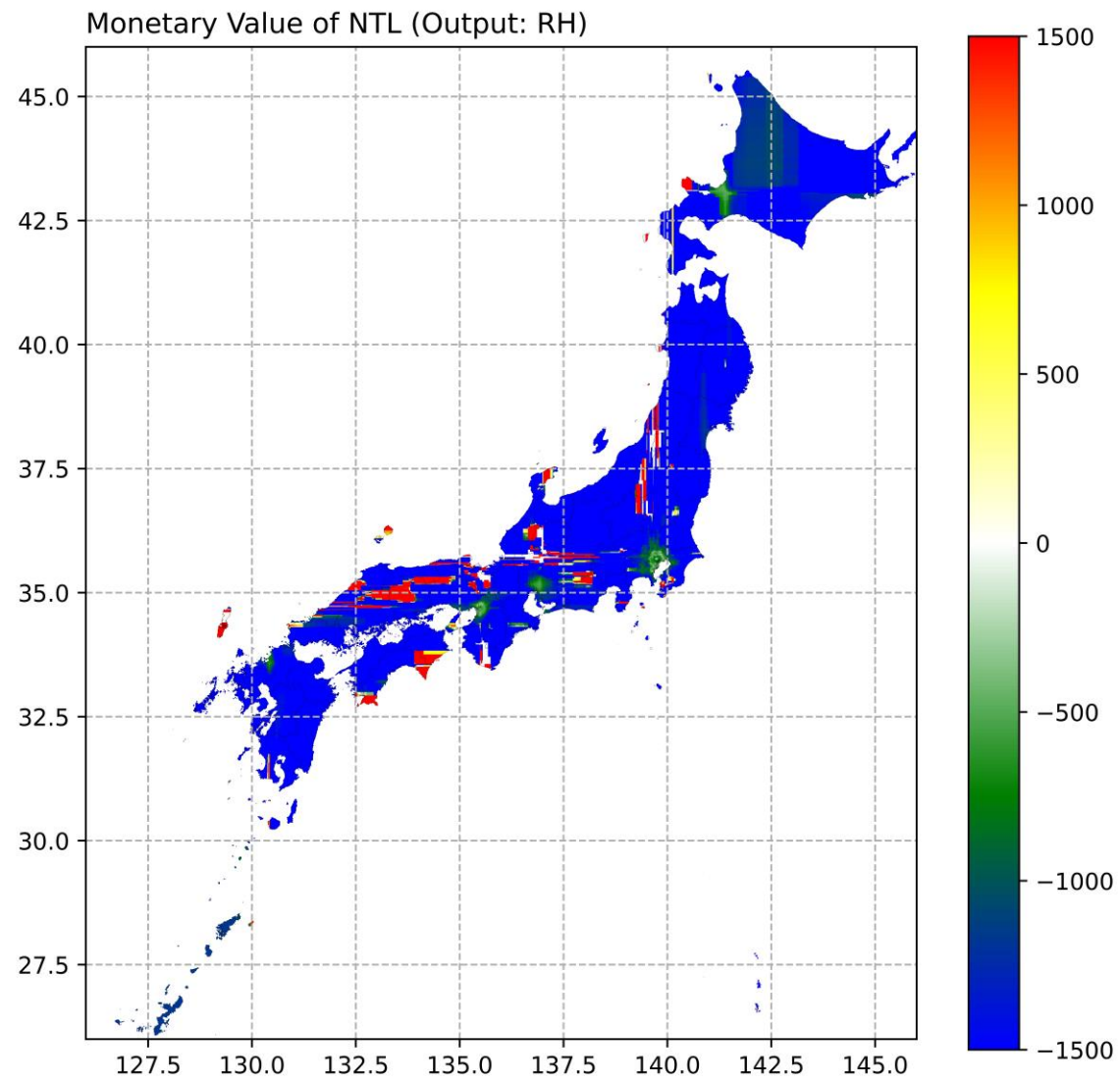
Figure 28: The Monetary Value of NDVI on RLS (unit: $\text{USD}/(\text{nW}/\text{cm}^2 \cdot \text{sr})$)

745



746

Figure 29: The Monetary Value of NDVI on OH (unit: $\text{USD}/(nW/cm^2 \cdot sr)$)



747

748

Figure 30: The Monetary Value of NDVI on RH (unit: $\text{USD}/(nW/cm^2 \cdot sr)$)

749

750

751

752

753

754

755

756

757

758

759 **Reference:**

- 760 Akpinar, A., Barbosa-Leiker, C., & Brooks, K.R. (2016). Does green space matter?
761 Exploring relationships between green space type and health indicators. *Urban Forestry &*
762 *Urban Greening*, 20, 407-418
- 763 Ambrey, C., & Fleming, C. (2014). Public Greenspace and Life Satisfaction in Urban
764 Australia. *Urban Studies*, 51, 1290-1321
- 765 Astell-Burt, T., & Feng, X. (2019). Association of Urban Green Space With Mental Health
766 and General Health Among Adults in Australia. *JAMA Network Open*, 2, e198209
- 767 Astell-Burt, T., Mitchell, R., & Hartig, T. (2014). The association between green space and
768 mental health varies across the lifecourse. A longitudinal study. *Journal of Epidemiology*
769 and *Community Health*, 68, 578-583
- 770 Barton, J., & Pretty, J. (2010). What is the Best Dose of Nature and Green Exercise for
771 Improving Mental Health? A Multi-Study Analysis. *Environmental Science & Technology*,
772 44, 3947-3955
- 773 Beenstock, M., & Felsenstein, D. (2019). *The econometric analysis of non-stationary*
774 *spatial panel data*. Springer
- 775 Begou, P., Kassomenos, P., & Kelessis, A. (2020). Effects of road traffic noise on the
776 prevalence of cardiovascular diseases: The case of Thessaloniki, Greece. *Science of The*
777 *Total Environment*, 703, 134477
- 778 Bertram, C., & Rehdanz, K. (2015). The role of urban green space for human well-being.
779 *Ecological Economics*, 120, 139-152
- 780 Bratman, G.N., Anderson, C.B., Berman, M.G., Cochran, B., de Vries, S., Flanders, J.,
781 Folke, C., Frumkin, H., Gross, J.J., Hartig, T., Kahn, P.H., Kuo, M., Lawler, J.J., Levin,
782 P.S., Lindahl, T., Meyer-Lindenberg, A., Mitchell, R., Ouyang, Z.Y., Roe, J., Scarlett, L.,
783 Smith, J.R., van den Bosch, M., Wheeler, B.W., White, M.P., Zheng, H., & Daily, G.C.
784 (2019). Nature and mental health: An ecosystem service perspective. *Science Advances*, 5,
785 eaax0903
- 786 Breiman, L. (2001). Random Forests. *Machine Learning*, 45, 5-32
- 787 Breiman, L., Friedman, J.H., Olshen, R.A., & Stone, C.J. (2017). Classification And
788 Regression Trees
- 789 Chameides, W.L., Lindsay, R.W., Richardson, J., & Kiang, C.S. (1988). The role of
790 biogenic hydrocarbons in urban photochemical smog: Atlanta as a case study. *Science*, 241,
791 1473-1475
- 792 Chapman, A., Fujii, H., & Managi, S. (2019). Multinational life satisfaction, perceived
793 inequality and energy affordability. *Nature Sustainability*, 2, 508-514
- 794 Chen, X., & Nordhaus, W.D. (2011). Using luminosity data as a proxy for economic
795 statistics, 108, 8589-8594
- 796 Chen, X., & Nordhaus, W.D. (2019). VIIRS Nighttime Lights in the Estimation of Cross-
797 Sectional and Time-Series GDP. *Remote Sensing*, 11, 1057
- 798 Chen, Z., Yu, B., Yang, C., Zhou, Y., Yao, S., Qian, X., Wang, C., Wu, B., & Wu, J. (2021).
799 An extended time series (2000–2018) of global NPP-VIIRS-like nighttime light data from
800 a cross-sensor calibration. *Earth System Science Data*, 13, 889-906
- 801 Didan, K., Munoz, A.B., Solano, R., Huete, A., & University of Arizona: Vegetation Index
802 Phenology Lab (2015). MODIS vegetation index user's guide (MOD13 series). In
- 803 Diener, E. (1984). Subjective well-being. *Psychological Bulletin*, 95, 542-575

- 804 Diener, E., Oishi, S., & Tay, L. (2018). Advances in subjective well-being research. *Nature*
805 *Human Behaviour*, 2, 253-260
- 806 Eitelberg, D.A., Van Vliet, J., Doelman, J.C., Stehfest, E., & Verburg, P.H. (2016).
807 Demand for biodiversity protection and carbon storage as drivers of global land change
808 scenarios, 40, 101-111
- 809 Falchi, F., Cinzano, P., Elvidge, C.D., Keith, D.M., & Haim, A. (2011). Limiting the impact
810 of light pollution on human health, environment and stellar visibility. *Journal of*
811 *Environmental Management*, 92, 2714-2722
- 812 Falchi, F., Furgoni, R., Gallaway, T.A., Rybnikova, N.A., Portnov, B.A., Baugh, K.,
813 Cinzano, P., & Elvidge, C.D. (2019). Light pollution in USA and Europe: The good, the
814 bad and the ugly. *Journal of Environmental Management*, 248, 109227
- 815 Felipe-Lucia, M.R., Soliveres, S., Penone, C., Manning, P., van der Plas, F., Boch, S., Prati,
816 D., Ammer, C., Schall, P., Gossner, M.M., Bauhus, J., Buscot, F., Blaser, S., Bluthgen, N.,
817 de Frutos, A., Ehbrecht, M., Frank, K., Goldmann, K., Hansel, F., Jung, K., Kahl, T., Nauss,
818 T., Oelmann, Y., Pena, R., Polle, A., Renner, S., Schloter, M., Schonning, I., Schrumpf, M.,
819 Schulze, E.D., Solly, E., Sorkau, E., Stempfhuber, B., Tschapka, M., Weisser, W.W.,
820 Wubet, T., Fischer, M., & Allan, E. (2018). Multiple forest attributes underpin the supply
821 of multiple ecosystem services. *Nature Communications*, 9, 4839
- 822 Fotheringham, A., Brunsdon, C., & Charlton, M. (2002). *Geographically Weighted*
823 *Regression: The Analysis of Spatially Varying Relationships*. John Wiley & Sons
- 824 Friedman, J.H. (2001). Greedy Function Approximation: A Gradient Boosting Machine.
825 *The Annals of Statistics*, 29, 1189-1232
- 826 Gaston, K.J., Gaston, S., Bennie, J., & Hopkins, J. (2015). Benefits and costs of artificial
827 nighttime lighting of the environment. *Environmental Reviews*, 23, 14-23
- 828 Ghosh, T., Anderson, S., Elvidge, C., & Sutton, P. (2013). Using Nighttime Satellite
829 Imagery as a Proxy Measure of Human Well-Being. *Sustainability*, 5, 4988-5019
- 830 Greenwell, B.M. (2017). pdp: an R Package for constructing partial dependence plots. *R*
831 *Journal*, 9, 421
- 832 Hartig, T., & Kahn, P.H. (2016). Living in cities, naturally. *Science*, 352, 938-940
- 833 Hothorn, T., Hornik, K., & Zeileis, A. (2006). Unbiased Recursive Partitioning: A
834 Conditional Inference Framework. *Journal of Computational and Graphical Statistics*, 15,
835 651-674
- 836 Hunter, R.F., Christian, H., Veitch, J., Astell-Burt, T., Hipp, J.A., & Schipperijn, J. (2015).
837 The impact of interventions to promote physical activity in urban green space: A systematic
838 review and recommendations for future research. *Social Science & Medicine*, 124, 246-
839 256
- 840 Kahneman, D., Krueger, A.B., Schkade, D.A., Schwarz, N., & Stone, A.A. (2004). A
841 Survey Method for Characterizing Daily Life Experience: The Day Reconstruction Method.
842 *Science*, 306, 1776-1780
- 843 Krekel, C., Kolbe, J., & Wuestemann, H. (2016). The greener, the happier? The effect of
844 urban land use on residential well-being. *Ecological Economics*, 121, 117-127
- 845 Lamchin, M., Lee, W.-K., Jeon, S.W., Wang, S.W., Lim, C.H., Song, C., & Sung, M.
846 (2018). Long-term trend and correlation between vegetation greenness and climate
847 variables in Asia based on satellite data. *Science of The Total Environment*, 618, 1089-
848 1095

- 849 Li, C., & Managi, S. (2021a). Contribution of on-road transportation to PM2.5. *Scientific*
850 *Reports*, 11, 21320
- 851 Li, C., & Managi, S. (2021b). Land cover matters to human well-being. *Scientific Reports*,
852 11
- 853 Li, C., & Managi, S. (2021c). Spatial Variability of the Relationship between Air Pollution
854 and Well-being. *Sustainable Cities and Society*, 103447
- 855 Li, C., & Managi, S. (2022). Estimating monthly global ground-level NO₂ concentrations
856 using geographically weighted panel regression. *Remote Sensing of Environment*, 280,
857 113152
- 858 Li, W., Saphores, J.D.M., & Gillespie, T.W. (2015). A comparison of the economic
859 benefits of urban green spaces estimated with NDVI and with high-resolution land cover
860 data. *Landscape and Urban Planning*, 133, 105-117
- 861 Liaw, A., & Wiener, M. (2002). Classification and regression by randomForest. *R News*,
862 2, 18-22
- 863 Lundberg, S.M., Erion, G., Chen, H., Degrave, A., Prutkin, J.M., Nair, B., Katz, R.,
864 Himmelfarb, J., Bansal, N., & Lee, S.-I. (2020). From local explanations to global
865 understanding with explainable AI for trees. *Nature Machine Intelligence*, 2, 56-67
- 866 Lundberg, S.M., & Lee, S.-I. (2017). A unified approach to interpreting model predictions.
867 *Advances in neural information processing systems*, 30
- 868 MacKerron, G. (2012). Happiness Economics from 35 000 Feet. *Journal of Economic*
869 *Surveys*, 26, 705-735
- 870 MacKerron, G., & Mourato, S. (2013). Happiness is greater in natural environments.
871 *Global Environmental Change*, 23, 992-1000
- 872 McCallum, I., Kyba, C.C.M., Bayas, J.C.L., Moltchanova, E., Cooper, M., Cuaresma, J.C.,
873 Pachauri, S., See, L., Danylo, O., Moorthy, I., Lesiv, M., Baugh, K., Elvidge, C.D., Hofer,
874 M., & Fritz, S. (2022). Estimating global economic well-being with unlit settlements.
875 *Nature Communications*, 13
- 876 Mendoza-Ponce, A., Corona-Núñez, R., Kraxner, F., Leduc, S., & Patrizio, P. (2018).
877 Identifying effects of land use cover changes and climate change on terrestrial ecosystems
878 and carbon stocks in Mexico. *Global Environmental Change*, 53, 12-23
- 879 Molnar, C. (2020). *Interpretable machine learning*. Lulu. com
- 880 Oswald, A.J., & Wu, S. (2010). Objective Confirmation of Subjective Measures of Human
881 Well-Being: Evidence from the USA. *Science*, 327, 576-579
- 882 Pirrera, S., De Valck, E., & Cluydts, R. (2010). Nocturnal road traffic noise: A review on
883 its assessment and consequences on sleep and health. *Environment International*, 36, 492-
884 498
- 885 Ryff, C.D. (2014). Psychological Well-Being Revisited: Advances in the Science and
886 Practice of Eudaimonia. *Psychotherapy and Psychosomatics*, 83, 10-28
- 887 Schapire, R.E. (2003). The Boosting Approach to Machine Learning: An Overview. (pp.
888 149-171): Springer New York
- 889 Seresinhe, C.I., Preis, T., & Moat, H.S. (2015). Quantifying the Impact of Scenic
890 Environments on Health. *Scientific Reports*, 5, 16899
- 891 Steptoe, A., Deaton, A., & Stone, A.A. (2015). Subjective wellbeing, health, and ageing.
892 *The Lancet*, 385, 640-648

- 893 Suk, J.Y., & Walter, R.J. (2019). New nighttime roadway lighting documentation applied
894 to public safety at night: A case study in San Antonio, Texas. *Sustainable Cities and Society*,
895 46, 101459
- 896 Triguero-Mas, M., Dadvand, P., Cirach, M., Martinez, D., Medina, A., Mompart, A.,
897 Basagana, X., Grazuleviciene, R., & Nieuwenhuijsen, M.J. (2015). Natural outdoor
898 environments and mental and physical health: Relationships and mechanisms.
899 *Environment International*, 77, 35-41
- 900 Tsurumi, T., Imauji, A., & Managi, S. (2018). Greenery and Subjective Well-being:
901 Assessing the Monetary Value of Greenery by Type. *Ecological Economics*, 148, 152-169
- 902 Wang, R., Yang, B., Yao, Y., Bloom, M.S., Feng, Z., Yuan, Y., Zhang, J., Liu, P., Wu, W.,
903 Lu, Y., Baranyi, G., Wu, R., Liu, Y., & Dong, G. (2020). Residential greenness, air
904 pollution and psychological well-being among urban residents in Guangzhou, China.
905 *Science of The Total Environment*, 711, 134843
- 906 White, M.P., Alcock, I., Wheeler, B.W., & Depledge, M.H. (2013). Would You Be Happier
907 Living in a Greener Urban Area? A Fixed-Effects Analysis of Panel Data. *Psychological
908 Science*, 24, 920-928
- 909 Yeh, C., Perez, A., Driscoll, A., Azzari, G., Tang, Z., Lobell, D., Ermon, S., & Burke, M.
910 (2020). Using publicly available satellite imagery and deep learning to understand
911 economic well-being in Africa. *Nature Communications*, 11
- 912 Zhao, N.Z., Liu, Y., Cao, G.F., Samson, E.L., & Zhang, J.Q. (2017). Forecasting China's
913 GDP at the pixel level using nighttime lights time series and population images. *Giscience
914 & Remote Sensing*, 54, 407-425
- 915 Zhao, Y., Qu, Z., Zhang, Y., Ao, Y., Han, L., Kang, S., & Sun, Y. (2022). Effects of human
916 activity intensity on habitat quality based on nighttime light remote sensing: A case study
917 of Northern Shaanxi, China. *Science of The Total Environment*, 851, 158037

918

919

920 **Appendix:**

Table S1: Descriptive Statistics of Features

Statistic	N	Mean	St. Dev.	Min	Pctl(25)	Pctl(75)	Max
OVLS	383,173	3.38	0.95	1	3	4	5
OH	383,173	3.61	0.91	1	3	4	5
RLS	383,173	3.14	0.94	1	3	4	5
RH	383,173	3.38	0.89	1	3	4	5
Individual Income	383,173	4.69	3.90	1	1	6.5	30
NDVI	383,173	36.25	13.66	4.86	26.26	44.25	87.71
NTL	383,173	18.59	15.86	0.01	6.04	26.74	88.81
Year	383,173	2015.66	0.77	2015	2015	2016	2017
Latitude	383,173	35.71	2.13	24.30	34.75	35.81	45.51
Longitude	383,173	137.52	3.05	123.76	135.55	139.72	145.74
Female Dummy (Gender)	383,173	0.35	0.48	0	0	1	1
Age	383,173	48.97	11.73	17	41	57	101
Frequency of High-level Stress	383,173	3.17	1.17	1	2	4	5
Frequency of Low-level Stress	383,173	3.61	1.06	1	3	4	5
Easy to Relax	383,173	3.29	1.02	1	3	4	5
Sense of Goodness for Living	383,173	3.83	0.90	1	3	4	5
Safe Feeling of Living Environments	383,173	2.95	0.76	0	3	3	4
Community Attachment	383,173	3.32	1.03	1	3	4	5
Income Level	383,173	4.04	2.87	1	1	6	13
Self-reported Health	383,173	3.25	1.27	1	2	4	5
Student Dummy	383,173	0.01	0.11	0	0	0	1
Worker Dummy	383,173	0.60	0.49	0	0	1	1
Company Owner Dummy	383,173	0.02	0.16	0	0	0	1
Government Officer Dummy	383,173	0.05	0.22	0	0	0	1
Self-employed Dummy	383,173	0.07	0.26	0	0	0	1
Professional Job Dummy	383,173	0.03	0.16	0	0	0	1
Housewife Dummy	383,173	0.09	0.28	0	0	0	1
Retired Dummy	383,173	0.06	0.25	0	0	0	1

Unemployed Dummy	383,173	0.05	0.21	0	0	0	1
College without Diploma	383,173	0.21	0.41	0	0	0	1
Bachelor Dummy	383,173	0.44	0.50	0	0	1	1
Master Dummy	383,173	0.05	0.21	0	0	0	1
PhD Dummy	383,173	0.01	0.12	0	0	0	1

921

922